POLITECNICO DI TORINO



Master Degree course in Automotive Engineering

Master Degree Thesis

Vertical and Longitudinal Dynamics Control in In-Wheel Motor Electric Vehicles

Supervisors

Prof. TONOLI ANDREA

Dr. SORRENTINO GENNARO

Dr. RAFFAELE MANCA

Candidate YU HUANG

Abstract

Adding electric motors straight to the wheel hub of a vehicle can improve its handling performance, consume less energy, and give designers more options when it comes to vehicle design. The removal of traditional drivetrain parts makes it possible for better torque control by in-wheel motors (IWMs). In terms of acceleration, braking, pitching, and heaving, this affects the vehicle's dynamics in both the longitudinal and vertical directions. With the help of integrated controller modulation, this study looks into how In-Wheel Motors (IWMs) affect the vertical and longitudinal dynamics of cars. using real-time data over the simulation time from the car's body and wheels, the suspension system makes dynamic adjustments to improve ride comfort and stability.

Hybrid, Skyhook, Groundhook, and longitudinal PID torque controllers are built into a quarter-car Simulink model. To enhance passenger comfort, the Skyhook device keeps the acceleration of sprung mass to a relatively low value. Groundhook minimizes tire load variations, thereby enhancing road-holding capabilities. The Hybrid controller optimizes the balance between comfort and handling. Performance is evaluated against a passive suspension system. Testing performed on uneven terrain, ISO 8608 class C road and road with impulse-like bumps, road surfaces with differing friction coefficients (spanning from 0.8 to 0.17) demonstrates that the combination of vertical control and torque adjustments improves ride quality and vehicle handling. Skyhook focuses on enhancing passenger comfort, while Groundhook is designed to optimize road-holding performance, especially on low-friction surfaces. The results show that larger unsprung mass(IWM) operating with active controlling strategies significantly enhances electric vehicles' performance across a variety of road conditions.

Acknowledgements

I extend my highest respect to my parents for their selfless support, to Italy for being the land that shaped me, to my tutors for their invaluable guidance.

Contents

1	Intr	oduction	8
	1.1	Background	8
	1.2	Objectives of the Research	9
	1.3	Structure of the Thesis	0
2	Lite	rature Review 1	1
	2.1	Vehicle Dynamics in In-Wheel Motor EVs	1
		2.1.1 Impact of Increased Unsprung Mass on Ride Quality	1
		2.1.2 Importance of Longitudinal and Vertical Dynamics in Vehicle Per-	
			2
	2.2	The state of the s	3
	2.3	0	4
		1 0	4
		2.3.2 Active Suspension Systems	5
3	Me	hodology 1	6
	3.1	Overview	6
	3.2	Quarter-Car Model	7
		3.2.1 Quarter-Car Model: Inputs and Outputs	7
		3.2.2 Mathematical Models and Applications	0
	3.3	Pacejka '96 Magic Formula	22
		3.3.1 Slip Ratio Definition	4
		3.3.2 Integration with Vehicle Dynamics	4
		3.3.3 Illustrative Force-Slip Curve	4
		3.3.4 Applications in In-Wheel Motor Vehicles	4
	3.4	Road Profiles	25
		3.4.1 ISO 8608 Class C Road	25
		3.4.2 Four Bumps Road Profile	6
	3.5	Road Profile Enveloping Model and Simulation Scenarios	7
	3.6	Controllers Design	8
		3.6.1 Longitudinal Slip Controller	28
		3.6.2 Vertical Active Controllers: Skyhook, Groundhook, and Hybrid 3	0
	Key Performance Indicators (KPIs)	3	
		3.7.1 Sprung-Mass Weighted Vertical Acceleration	3

		3.7.2	Road-Holding Index (RHI)	34
		3.7.3	Maximum Tire Slip	34
		3.7.4	Slip Error Integral	35
		3.7.5	Summary of KPIs	35
	3.8	Vehicle	e Parameters	35
4	Res	ults an	nd Discussion	36
	4.1	ISO 86	608 Class C Road with Constant Friction Coefficient (μ)	36
		4.1.1	Comfort Analysis	36
		4.1.2	Handling Performance	36
		4.1.3	Stability and Slip Control	37
		4.1.4	Implications for Control Strategies	37
	4.2	ISO 86	608 Class C Road with Variable Friction Coefficient (μ)	36
		4.2.1	Ride Comfort Analysis	40
		4.2.2	Handling Performance	40
		4.2.3	Stability and Slip Control	40
		4.2.4	Implications for Control Strategy Selection	41
		4.2.5	Frequency Domain Response Analysis	41
		4.2.6	Energy Consumption for Control Strategy Selection	41
	4.3	Four E	Bumps Road with Variable Friction Coefficient (μ)	45
		4.3.1	Ride Comfort Analysis	46
		4.3.2	Handling Performance	47
		4.3.3	Stability and Slip Control	47
		4.3.4	Implications for Control Strategy Selection	47
		4.3.5	Frequency Domain Response Analysis	47
		4.3.6	Energy Consumption for Control Strategy Selection	48
5	Con	clusio	n and Future Work	52
	5.1	Summ	ary of Findings	52
	5.2	Future	e Research Directions	53
		5.2.1	Development of More Complex and High-Fidelity Vehicle Models .	53
		5.2.2	Advanced Control Techniques	53
		5.2.3	Integrated Longitudinal and Vertical Dynamics Control	53
		5.2.4	Experimental Validation and Real-Time Implementation	54
		5 2 5	Summary	54

List of Figures

1.1	Schematic of an in-wheel motor integrated into the wheel hub (adapted from Biček et al. [4])	8
1.2	Increased unsprung mass with active suspension system	9
2.1	Schematic of suspension dynamics showing the interaction between unsprung mass, suspension, and vehicle body motion	11
2.2	Relationship between slip ratio λ and friction coefficient (adapted from "A robust slip based traction control of electric vehicle under different road conditions" [26])	14
3.1	Overview of the Simulink quarter-car model with in-wheel motor integration and external inputs	16
3.2	Quarter-car model schematic including sprung and unsprung masses, suspension, tire, and external forces (adapted from IEEE document [24])	17
3.3	Pacejka '96 model [19]. The curve illustrates linear, nonlinear, and saturation regions relevant for traction and braking control	23
3.4	Illustration of the longitudinal tire force as a function of slip ratio based on the Pacejka '96 model [19]. The curve illustrates linear, nonlinear, and saturation regions relevant for traction and braking control	25
3.5	ISO 8608 Class C road profile used in simulations	26
3.6	Four-bump road profile with varying friction.	27
3.7	Schematic of the longitudinal slip control loop implemented in Simulink.	29
3.8	Root locus of the longitudinal PID controller showing closed-loop pole trajectories	29
3.9	Bode plot of the PID controller demonstrating frequency response characteristics	30
3.10	Block diagram of active Skyhook controller	30
	schematic of active Skyhook controller	31
	Block diagram of active Groundhook controller	31
	schematic of active Groundhook controller.	32
	Block diagram of active Hybrid controller combining Skyhook and Ground-	
9 1 5	hook logic	32
3.1 3	schematic of active Hybrid controller.	33
4.1	Comparison of slip with and without IWM	37

$List\ of\ Figures$

4.2	Comparison of sprung mass vertical acceleration with and without IWM . 3
4.3	Comparison of $z_u - w$ with and without IWM
4.4	ISO road – Wheel Slip Ratio
4.5	ISO road – Body Longitudinal Velocity (x_{bd})
4.6	ISO road – Motor Torque
4.7	ISO road – Sprung Mass Acceleration responses
4.8	ISO road – Active Force responses
4.9	ISO road – Suspension Travel responses
4.10	ISO road – Power and Energy Consumption
4.11	Four Bumps Road – Wheel Slip Ratio
4.12	Four Bumps Road – Body Longitudinal Velocity (x_{bd}) 4
4.13	Four Bumps Road – Motor Torque
4.14	Four Bumps Road – Sprung Mass Acceleration
4.15	Four Bumps Road – Active Force
4.16	Four Bumps Road – Suspension Travel
4.17	Four-bumps road – Power and Energy Consumption responses

List of Tables

3.1	Quarter-Car Model Inputs and Outputs	19
3.2	Input variables for the Pacejka '96 longitudinal model	23
3.3	Outputs of the Pacejka '96 longitudinal model	23
3.4	Key Performance Indicators for Vehicle Evaluation	35
3.5	Vehicle parameters used in the simulation	35
4.1	Influence of Increased Unsprung Mass on Vehicle Performance (ISO Class	
	C Road, Variable μ)	40
4.2	Energy Consumption Comparison (ISO Class C Road, Variable μ)	40
4.3	Influence of Increased Unsprung Mass on Vehicle Performance (Four Bumps	
	Road, Variable μ)	46
4.4	Energy Consumption Comparison (3cm Bumps Road)	

Chapter 1

Introduction

1.1 Background

The use of in-wheel motors (IWMs) (figure 1.1) in electric vehicles can increase energy efficiency and provide designers with more flexibility. Embedding the motor in the wheel hub eliminates components such as axles and half-shafts, facilitating precise torque control for each wheel.

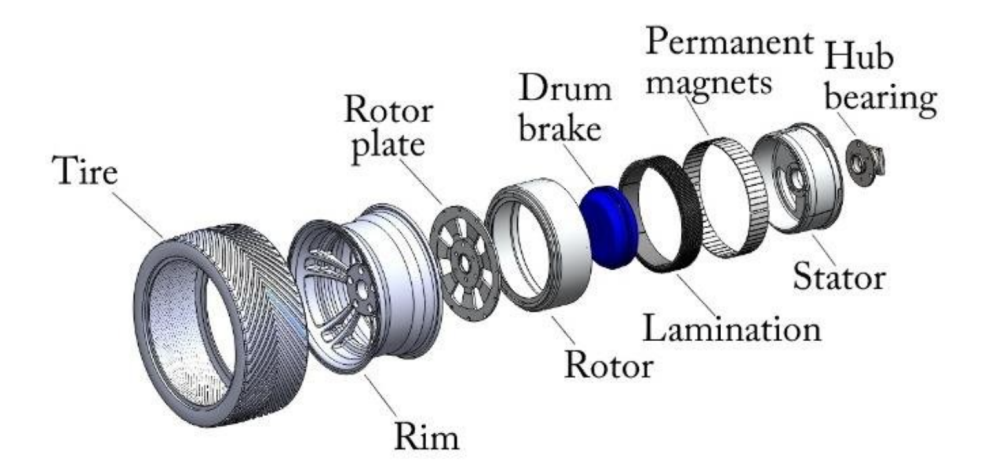


Figure 1.1: Schematic of an in-wheel motor integrated into the wheel hub (adapted from Biček et al. [4]).

However, IWMs increase the vehicle's unsprung mass. This extra weight on the wheel makes it harder for the suspension to absorb bumps on the road, which could make the ride less comfortable and stable. Figure 1.2 shows an active suspension system that can help to reduce those negative effects due to extra unsprung mass.



Figure 1.2: Increased unsprung mass with active suspension system.

1.2 Objectives of the Research

This study looks into how vehicles with In-Wheel Motors (IWMs) behave vertically and longitudinally, focusing on how an extra unsprung mass impacts ride comfort and handling. Here are a list of the goals:

- Developing a quarter-car simulation model with IWMs to evaluate an automobile's response to various road profiles.
- Using damping control techniques to make the ride more comfortable and help the vehicle stay on the road when the unsprung mass is high.
- Comparing different suspension control strategies (Skyhook, Groundhook and Hybrid) and PID controller for overall dynamic performance, comfort, and traction.
- Looking at the results and benefits of ride comfort and vehicle stability in a range of different road conditions and values of friction.

1.3 Structure of the Thesis

The thesis is structured in the following manner:

- Chapter 2: Literature Review Talks about IWMs, the mechanics of vehicles moving in vertical and longitudinal directions, and different control methods (Skyhook, Groundhook, and Hybrid), focusing on how unsprung mass affects performance.
- Chapter 3: Methodology Presents the quarter-car model, the tire model, the IWM integration, the torque modulation design, and controlling performance metrics.
- Chapter 4: Results and Discussion Results of the simulation that compared active controllers to passive approaches, focusing on ride comfort, road-holding, and sliding dynamics.
- Chapter 5: Conclusion and Future Work This part sums up the results and talks about what they mean for the design of electric vehicles in real-world situations and for future research.

Chapter 2

Literature Review

2.1 Vehicle Dynamics in In-Wheel Motor EVs

2.1.1 Impact of Increased Unsprung Mass on Ride Quality

The unsprung mass includes the items that the suspension springs do not support, such as wheels, brakes, and uprights. More unsprung mass means more inertia, which makes the wheels respond slowly to changes in the road. This can make the tires lose connection to the road and ability to hold on. Ride comfort gets worse because high-frequency vibrations are sent to the cabin more strongly. To lessen these effects, suggestions are given by using advanced active or semi-active suspension systems.

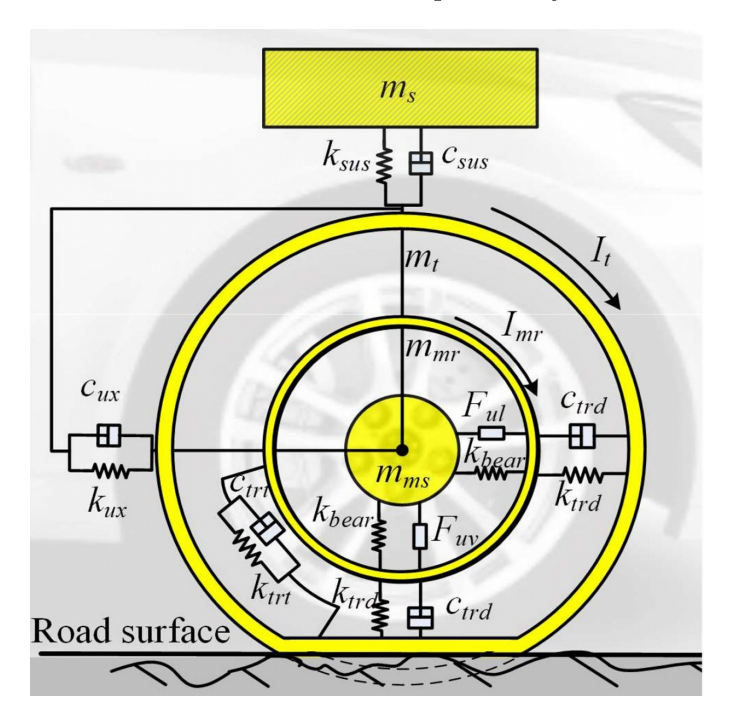


Figure 2.1: Schematic of suspension dynamics showing the interaction between unsprung mass, suspension, and vehicle body motion.

2.1.2 Importance of Longitudinal and Vertical Dynamics in Vehicle Performance

Vehicle dynamics includes longitudinal movements like acceleration and braking, along with vertical motions that pertain to ride comfort and road handling. In electric vehicles with built-in IWM, there exists a notable relationship between these two aspects, as the properties of wheel-end actuators and unsprung mass directly influence suspension performance and body accelerations. The mass of traditional cars is affect by the engine propulsion system. IWMs, on the other hand, move additional mass to the unsprung side, which changes the balanced dynamics [11, 25, 18].

Vertical Dynamics and Ride Quality

The way the car body reacts to bumps on the road is controlled by vertical dynamics. The suspension's ability to isolate influence of wheels is less effective when the unsprung mass become larger. Hrovat (1988) demonstrated that unsprung weight significantly influences ride quality and may restrict the advantages of active suspensions [11]. IWM induced unsprung mass effects on sprung mass acceleration and wheel load changes were measured by Wu et al. (2024), who found that these effects were amplified in the low and mid-frequency ranges [25]. Shi et al. (2015) further established that a larger unsprung mass in IWMs significantly impacts ride comfort [23]. To tackle these negative affects, IWMs can be considered as vertical actuators to affect tire forces and influence body accelerations. Bunlapyanan et al. (2024) presented analytical frameworks for the simultaneous use of IWMs in propulsion and vertical force actuation [5]. Hybrid suspension strategies, combining Skyhook and Groundhook damping, have been modified for use in IWM-based vehicles. Samaroo et al. (2025) showed that combining dual vibration absorbers with semi-active dampers improves comfort and handling stability. [22].

- Vertical dynamics influence the car's interaction with the road, affecting both ride comfort and safety.
- An increase in unsprung mass elevates wheel hop frequencies, resulting in reduced suspension isolation effectiveness.
- Active suspension strategies, such as Skyhook, Groundhook and Hybrid, help reduce ride degradation caused by IWM.
- IWMs have the capability to actively influence tire forces, affecting body acceleration profiles.

Longitudinal Dynamics and Traction Performance

The dynamics over time influence how acceleration, braking, and traction are managed. Conventional architectures concentrate on drivetrain and torque delivery, while IWMs deliver torque directly to each wheel, which fundamentally changes how longitudinal control works. Nguyen et al. (2020) highlighted the need to consider wheel-end inertia, torque response, and coupled body dynamics for stability and control [18].

Braking safety is directly affected. Ammari et al. (2022) showed that torque allocation must account for load transfer and vertical forces to ensure optimal braking performance [2]. Without coordination, uneven braking and reduced deceleration efficiency may occur.

Implications for EVs with In-Wheel Motors

IWMs are good with respect to aspects in terms of comfort, safety, and overall performance [7] when they have vertical force control, active suspension, and independent wheel torque properly combined. To keep the ride quality and road holding stable in a variety of driving situations, control algorithms must take into account the increased unsprung mass.

2.2 Slip Control and PID Control

In-wheel motors (IWMs) give each wheel its own power, which makes longitudinal control very accurate. Managing wheel slip is a big part of car longitudinal dynamics. Wheel slip has a direct effect on traction, how well the brakes work, and how stable the vehicle is. When the relative speed between the tire and the road goes over a certain point, slip happens. This makes the tires less stable. IWMs are different from other types of drive-trains because they allow changing the slip at each wheel separately.

A PID (Proportional-Integral-Derivative) system is often used for slip management. The slip ratio σ is defined as:

$$\sigma = \frac{v_{\text{vehicle}} - \omega R}{v_{\text{vehicle}}} \tag{2.1}$$

where v_{vehicle} is the speed of the vehicle moving along a straight line, ω is the angular velocity of the wheel, and R is the diameter of the tire. The PID processor changes the wheel torque T_w all the time to keep the slip ratio close to the best value, which is σ_{opt} :

$$T_w(t) = K_p e(t) + K_i \int_0^t e(\tau)d\tau + K_d \frac{de(t)}{dt}$$
(2.2)

where $e(t) = \sigma(t) - \sigma_{\text{opt}}$ and K_p , K_i , K_d are the proportional, integral, and derivative gains, respectively. The proportional term fixes things right away, the integral term gets rid of steady-state error, and the derivative term lowers overshoot and swings.

Slip-based PID control can also include regenerative braking, which changes the power to get energy back while keeping the wheels on the ground. Independent wheel torque control also allows torque vectoring, which makes the rotation more stable by spreading spatial forces more evenly across wheels.

New research backs up the idea that combining PID-based or LQR slip control with models of how the car moves and steers makes it more stable and easier to control on a variety of road conditions. Figure. 2.2 shows that the torque correction on each wheel is necessary to keep the best grip under different road condition. This makes driving safe and efficient and allows for advanced longitudinal and lateral control strategies.

Among the main benefits of slip-PID control:

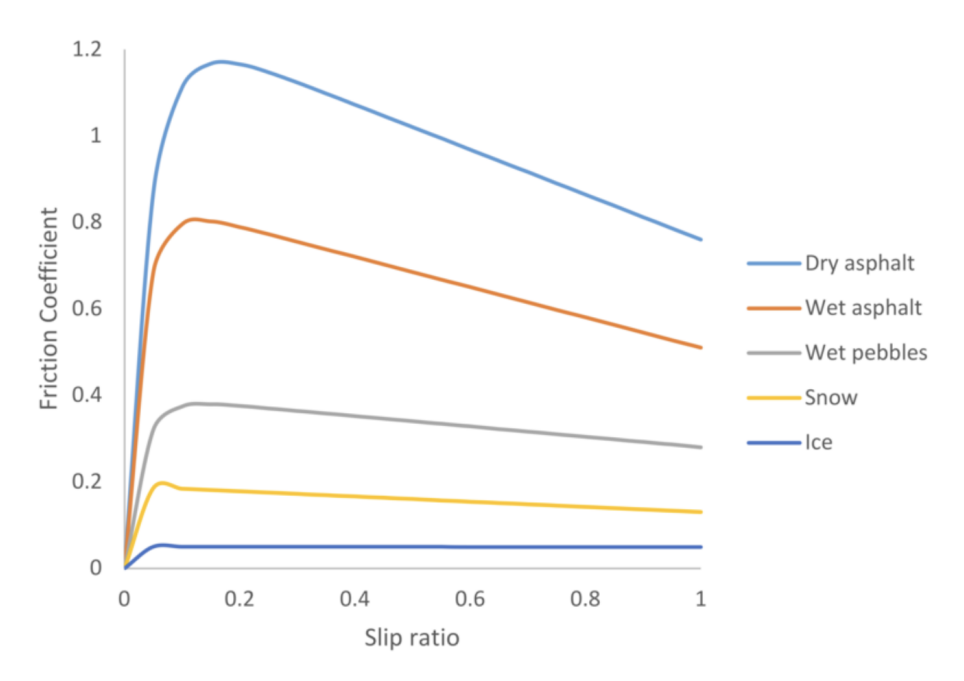


Figure 2.2: Relationship between slip ratio λ and friction coefficient (adapted from "A robust slip based traction control of electric vehicle under different road conditions" [26]).

- Provide better grip when speeding up or slowing down.
- Better safety when braking on areas with low friction.
- Energy recovery through coordinated regenerative braking.
- Foundation for torque vectoring and dynamic stability control.

2.3 Vertical Control Strategies

Vehicle vertical dynamics control is the priority for achieving a balance between ride comfort and handling stability. The suspension system is the core component, and its performance is determined by the active force control strategy. This part goes into detail about how passive and active suspension systems work, including how they can be represented mathematically and what problems they can cause in cars with in-wheel motors (IWMs).

2.3.1 Passive Damping

One of the solutions in automotive engineering is the passive suspension system, which is made up of a mechanical spring and a hydraulic damper. Its damping properties are fixed after manufacturing. The damping force F_d is modeled as a linear function of the damper's piston velocity v:

$$F_d = c \cdot v \tag{2.3}$$

where c is the constant damping coefficient.

Limitations with Increased Unsprung Mass

For in-wheel motor vehicles, the substantial increase in unsprung mass exacerbates the limitations of passive damping. The heavier wheel assembly generates higher inertia and larger amplitude oscillations. As a result:

- the tire contact force changes a lot, making the car less stable on the road.
- The cabin noises get worse, making the ride less comfortable.
- Traditional passive damping can not change in real time, which means that vibrations are suppressed later [15].

2.3.2 Active Suspension Systems

Active damping systems use controlled devices, like Electromagnetic or Pneumatic actuators, to get around the problems that passive damping systems have. Through control algorithms, their active force F(t) can be changed flexibly in milliseconds. Importantly, active dampers not only lose energy, but they can change the rate at which they lose energy in a smart way.

Control Strategies

Skyhook Control

As a way to improve passenger comfort, skyhook control reduces the movement of sprung mass. In a way, it acts like a virtual cushion between the sprung mass and a point of inertia, which we call "sky".

Groundhook Control

Groundhook control targets the unsprung mass to improve road-holding.

Hybrid Control

Hybrid control combines Skyhook and Groundhook strategies for a balanced performance.

Integration with In-Wheel Motors

In-wheel motor vehicles offer distinct advantages through active damping:

- The IWM delivers precise real-time input on wheel torque.
- The damping controller can align with longitudinal torque control, effectively reducing pitch and heave motions at the same time.
- The stability of the vehicle enhances when navigating through different road conditions [12].

Chapter 3

Methodology

3.1 Overview

In this thesis, a comprehensive Simulink model is developed to investigate the influence of unsprung mass on vehicle dynamics and to evaluate the effectiveness of active controlling strategies. The model is structured in modular structure, consisting of several core components: a motor torque source, a road profile generator, a quarter-car vehicle model (including detailed tire dynamics), and associated controllers. Figure 3.1 presents the overall architecture of the simulation framework, illustrating the interaction between vertical and longitudinal dynamics, tire-road contact, and control inputs.

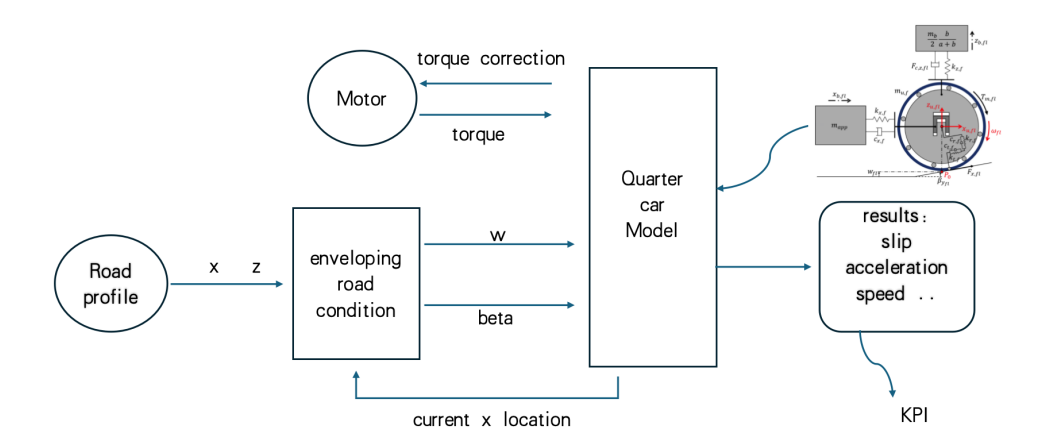


Figure 3.1: Overview of the Simulink quarter-car model with in-wheel motor integration and external inputs.

The framework is meant to give a accurate but also efficient computing model of a single wheel and how it interacts with the car body and the road surface. This can help us look closely at how the ride feels, how well the car handles, and how the tires slip on different types of roads and with different amounts of friction.

3.2 Quarter-Car Model

This model is often used to study vertical and longitudinal dynamics, suspension performance, and the relationship between tires and the road surface because the model is accurate and practical in simulation.

The system has a sprung mass (m_s) that sustains the body of the car, an unsprung mass (m_u) that sustains the wheels, and a suspension system with a spring (k_s) and damper (c_s) . Tire can be considered as a mix of linear stiffness (k_r) and damping (c_r) parts. Aerodynamic drag (F_{drag}) , rolling resistance (F_{roll}) , and road-induced vertical and horizontal excitations are some of the external forces that act on the system.

The design of the quarter-car model that was built is shown in Figure 3.2.

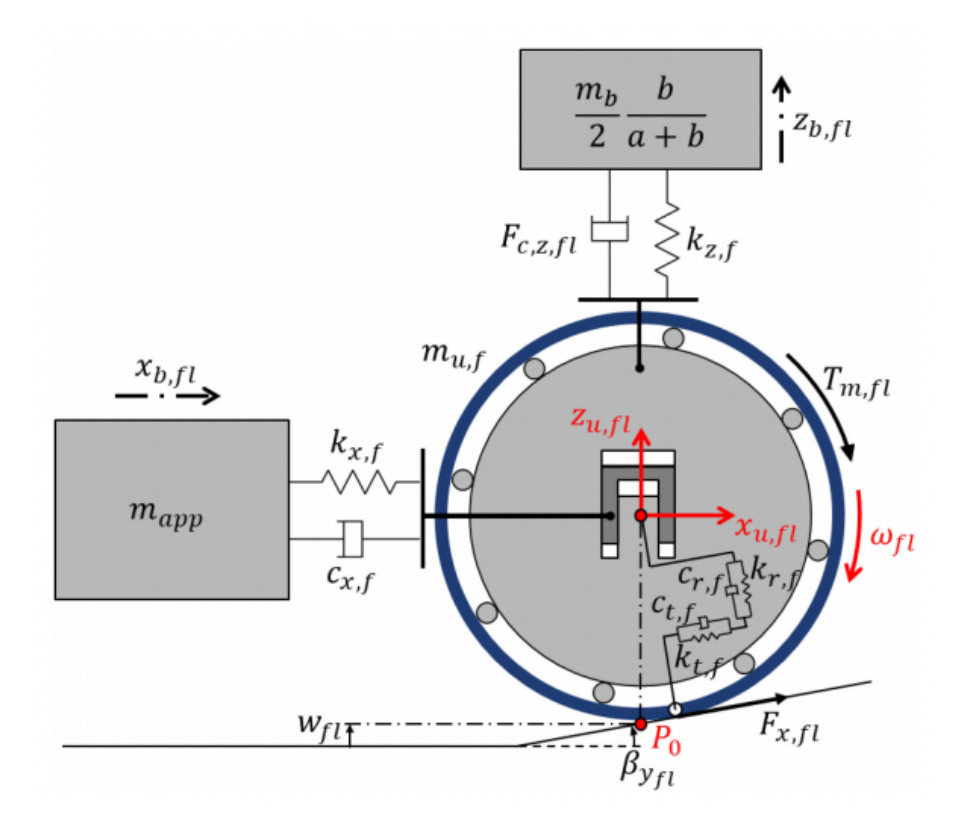


Figure 3.2: Quarter-car model schematic including sprung and unsprung masses, suspension, tire, and external forces (adapted from IEEE document [24]).

3.2.1 Quarter-Car Model: Inputs and Outputs

The quarter-car model takes information from the sensors, the vehicle's subsystems, and the motor inside the wheel. It then sends information back to the ECU that describes how the vehicle moves vertically and longitudinally, how the tires interact with the road, and how the wheels move. For reproducibility, controller design, and performance analysis, it is necessary to have a thorough list of all the inputs and outputs.

Inputs

The inputs to the quarter-car model can be sorted into four groups:

- 1. **Road Profile Inputs:** The road surface inputs can directly affect the tire's vertical and longitudinal forces.
 - W_r : Hollow, bumps, or other unevenness in the road's surface.
 - β : The angle of the road's slope, which changes how forces act on the tires' vertical and horizontal directions and how much weight is on each one.
- 2. Longitudinal and Vertical Forces: When the car body moves or when the suspension hits against on the wheel, forces from different direction push on the wheel suspension system.
 - F_x : longitudinal tire force, which is made up of forces from grip, stopping, and sliding.
 - F_z : The force hitting the tire straight on and being sent to the frame by the tire.
 - $F_k z, F_k x$: The force of the suspension spring and longitudinal spring, which can be found by seeing the length of the spring move when they are sprung and when they are not.
 - $F_c z$, $F_c x$: Suspension damper force and longitudinal damper, calculated from relative velocity between sprung and unsprung mass.
- 3. **In-Wheel Motor Torque:** There is a clear connection between the power that each in-wheel motor produces and the linear acceleration and wheel slip ratio.
 - T_m : Motor torque input (N·m), How much torque the wheel gets for acceleration depends on many things, like how heavy the car is and how well its tires grip the road.
- 4. **Vehicle and Suspension Parameters:** To acheive realistic dynamic models, it is necessary to know how the car's suspension system works physically.
 - m_s, m_u : Weights of the car, sprung and unsprung masses (kg).
 - k_s, c_s : Suspension's stiffness and damper factors, respectively.
 - k_r, c_r, k_t, c_t : stiffness and damping coefficients between IWM and wheel.
 - F_{drag} : Aerodynamic drag force, and it changes depending on how fast the car is going and how big its front end area is.
 - F_{roll} : Rolling resistance, the type of tire and the normal load determine the rolling resistance.

Outputs

The quarter-car model generates outputs that characterize the dynamic response of the vehicle and wheel system:

- 1. Sprung Mass Responses: Metrics related to the vehicle body's vertical motion.
 - z_b : Vertical displacement of the sprung mass.
 - \dot{z}_b : Vertical velocity.
 - \ddot{z}_b : Vertical acceleration, a primary indicator of ride comfort.
- 2. **Unsprung Mass Responses:** Wheel assembly vertical dynamics, critical for roadholding and contact stability.
 - z_u : Vertical displacement of the unsprung mass.
 - \dot{z}_u : Vertical velocity of the wheel assembly.
- 3. **Longitudinal Dynamics:** The motion of the vehicle in the direction of travel, which is pertinent to the assessment of acceleration, braking, and slip conditions.
 - x_b : Longitudinal displacement of the vehicle.
 - \dot{x}_b : Vehicle longitudinal velocity.
 - \ddot{x}_b : Longitudinal acceleration.
- 4. Tire Slip and Contact Forces: Parameters for how the wheel and road interact.
 - σ : The wheel slip ratio is the difference between the normalized speed of the wheel and the speed of the car.
 - F_x, F_z : Forces along the longitudinal and verticle direction of the tire at the contact patch.
 - ω : The angular speed of the wheel, which is found by looking at how the mass that is not sprung spins.

Table 3.1 summarizes the inputs and outputs for quick reference.

Table 3.1: Quarter-Car Model Inputs and Outputs

Inputs	Outputs
W_r, β	z_b,\dot{z}_b,\ddot{z}_b
$F_k z, F_c z, F_k x, F_c x$	$z_u, \dot{z}_u, x_u, \dot{x}_u$
F_x, F_z	$x_b, \dot{x}_b, \ddot{x}_b$
T_m	σ,ω
F_{drag}, F_{roll}	Tire-road contact forces

The detailed description shows how in-wheel motor vehicles interact with three different types of forces: vertical, longitudinal, and rotational. This approach makes it easy to add active suspension system, PID slip control, and hybrid control strategies to the simulation, which provides a dependable base for evaluating performance and choosing the best controller.

3.2.2 Mathematical Models and Applications

The quarter-car model functions as the basis for various performance assessments:

- Ride Comfort Analysis: Looking at the sprung mass's vertical acceleration (\ddot{z}_b) can help us figure out how the unsprung mass and different damping techniques affect passenger comfort.
- Vehicle Handling Study: Tire forces (F_x, F_z) and slip ratio (σ) are used to measure the vehicle's lengthwise stability and traction performance. The Road Holding Index (RHI) is used to measure how well a vehicle grips different types of road surface.

Quarter-Car Model Equations

The system consists of two distinct masses: the sprung mass (m_s) , which denotes the vehicle body, and the unsprung mass (m_u) , which corresponds to the wheel and brake components. The suspension system and tire are represented through the use of linear springs and dampers. Excitation from the road, aerodynamic drag, rolling resistance, and in-wheel motor torque are all examples of external forces.

Sprung Mass Vertical Motion

By Newton's second law of motion, the sprung mass vertical movements determined by:

$$\dot{z}_b = \frac{1}{m_s} \left(-F_{kz} - F_{cz} \right) \tag{3.1}$$

where the suspension spring and damping forces are defined as:

$$F_{kz} = k_{zf} \left(z_b - z_u \right) \tag{3.2}$$

$$F_{cz} = c_{zf} \left(\dot{z}_b - \dot{z}_u \right) \tag{3.3}$$

In this case, z_b and z_u show how the sprung and unsprung masses move up and down. k_{zf} and c_{zf} are the stiffness and dampening coefficients of the suspension. Equation (3.1) delineates the classical second-order response of the vehicle body subjected to vertical excitation.

Sprung Mass Longitudinal Motion

The longitudinal dynamics of the sprung mass account for in-wheel motor torque, suspension forces, and resistive forces:

$$\dot{x}_b = \frac{1}{m_{ann}} \left(-F_{kx} - F_{cx} + \frac{T_{m,frl}}{R} + \frac{T_{m,rrl}}{R} - F_{drag} - F_{roll} \right)$$
(3.4)

with longitudinal forces:

$$F_{kx} = k_{xf} \left(x_b - x_u \right) \tag{3.5}$$

$$F_{cx} = c_{xf} \left(\dot{x}_b - \dot{x}_u \right) \tag{3.6}$$

Aerodynamic drag and rolling resistance are:

$$F_{drag} = \frac{1}{2} \rho \, C_d \, A_f \, \dot{x}_b^2 \tag{3.7}$$

$$F_{roll} = \left(\frac{m_f * g}{2} + m_r * g\right) f_{roll} \tag{3.8}$$

Unsprung Mass Vertical Motion

The vertical dynamics of the unsprung mass account for suspension, tire forces, damping, and longitudinal interactions due to road slope:

$$\ddot{z}_{u} = \frac{1}{m_{u}} \left[F_{kz} - k_{r,f} (z_{u} - W_{f}) \cos^{2} \beta + k_{t,f} (z_{u} - W_{f}) \sin^{2} \beta - c_{r,f} (\dot{z}_{u} - \dot{W}_{f}) \cos^{2} \beta + c_{t,f} (\dot{z}_{u} - \dot{W}_{f}) \sin^{2} \beta + F_{cz} + F_{x} \sin \beta \right]$$
(3.9)

Unsprung Mass Longitudinal Motion

Longitudinal motion of the unsprung mass:

$$\ddot{x}_{u} = \frac{1}{m_{u}} \left[F_{kx} + F_{cx} + k_{r,f} (z_{u} - W_{f}) \sin \beta \cos \beta + k_{t,f} (z_{u} - W_{r}) \sin \beta \cos \beta + c_{r,f} (\dot{z}_{u} - \dot{W}_{f}) \sin \beta \cos \beta + c_{t,f} (\dot{z}_{u} - \dot{W}_{f}) \sin \beta \cos \beta + F_{x} \cos \beta \right]$$
(3.10)

Wheel Rotation Equation

The wheel rotational dynamics are captured by:

$$\dot{\omega} = \frac{1}{I_y} \left[T_{fl} - F_x R - \left(\frac{m_f * g}{2} f_{roll} R \right) \right]$$
 (3.11)

where I_y is the wheel rotational inertia, R is the wheel radius, T_{fl} is the applied motor torque, and F_x is the longitudinal tire force.

These equations collectively describe the coupled vertical, longitudinal, and rotational motions of the quarter-car system. They form the foundation for implementing active damping strategies, PID-based slip control, and integrated in-wheel motor torque modulation.

3.3 Pacejka '96 Magic Formula

The Pacejka '96 Magic Formula provides a semi-empirical approach to model tire forces and moments under various slip conditions. It is widely used in vehicle dynamics simulations due to its ability to capture the nonlinear relationship between tire slip and force. The general form of the Magic Formula is expressed as [19]:

$$Y = D \sin \left[C \arctan \left(BX - E(BX - \arctan(BX)) \right) \right]$$
 (3.12)

where:

- Y represents the tire output (force or moment),
- X denotes the input variable, such as slip ratio κ or slip angle α ,
- B is the stiffness factor,
- C is the shape factor,
- D is the peak factor, and
- E is the curvature factor.

For this thesis, the longitudinal behavior is relevant. Therefore, the longitudinal tire force equation, describing both braking and acceleration, is used:

$$F_x = D_x \sin \left[C_x \arctan \left(B_x \sigma - E_x (B_x \sigma - \arctan(B_x \sigma)) \right) \right]$$
(3.13)

$$F_y = D_y \sin \left[C_y \arctan \left(B_y \alpha - E_y (B_y \alpha - \arctan(B_y \alpha)) \right) \right]$$
 (3.14)

$$M_z = D_z \sin \left[C_z \arctan \left(B_z \alpha - E_z (B_z \alpha - \arctan (B_z \alpha)) \right) \right]$$
 (3.15)

Explanation of Variables

- F_x : Longitudinal tire force generated at the contact patch [N]
- σ : Slip ratio (dimensionless)
- B_x, C_x, D_x, E_x : Magic Formula coefficients for longitudinal behavior
- α : Tire slip angle (used in lateral modeling)
- F_y : Lateral force (not considered in current simulation)
- M_z : Self-aligning torque (not used in this thesis)

Model Inputs

The longitudinal Pacejka '96 model requires the following inputs:

Input	Description
$\overline{x_u}$	Unsprung mass vertical displacement
σ	Slip ratio (used to compute longitudinal force)
$F_{z,\mathrm{tire}}$	Vertical load on the tire (normal force)
μ	Road-tire friction coefficient
\dot{x}_b	Sprung mass longitudinal velocity
V_{cx}	Longitudinal vehicle speed used for parameter lookup
n-D $T(u)$	Nonlinear correction function or lookup table

Table 3.2: Input variables for the Pacejka '96 longitudinal model

Output	Description
$\overline{F_x}$	Longitudinal traction/braking force generated by the tire
$C_F k$	longitudinal slip stiffness (Fx slope in the origin)

Table 3.3: Outputs of the Pacejka '96 longitudinal model

Model Outputs

The model computes the following outputs:

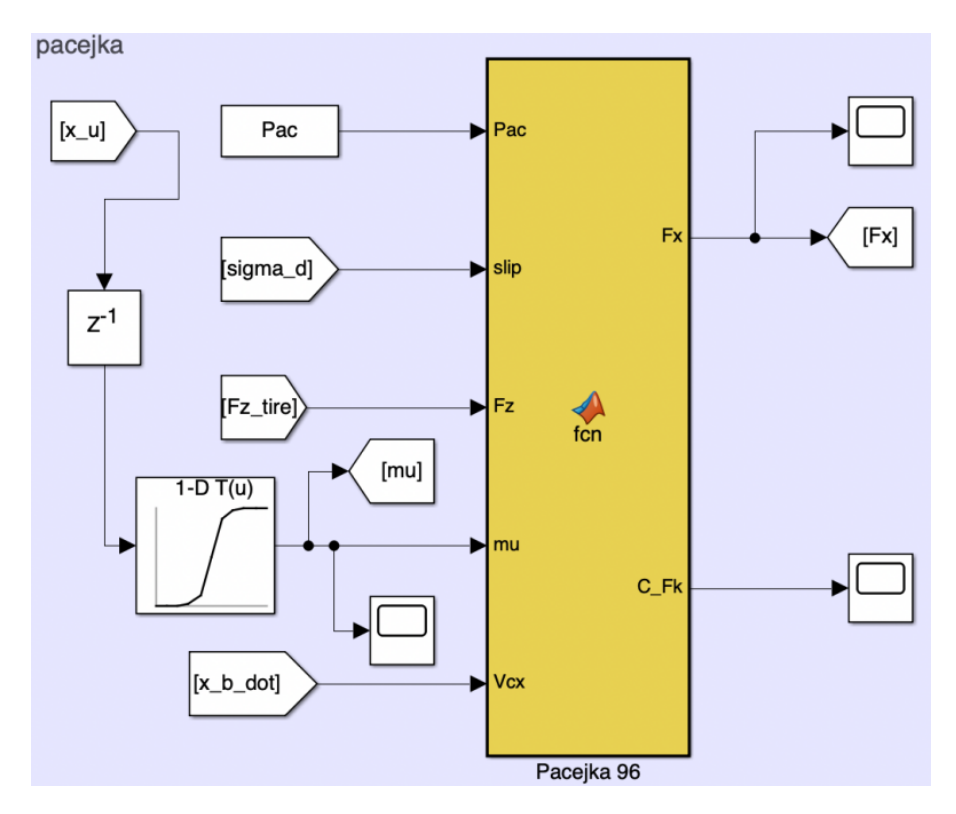


Figure 3.3: Pacejka '96 model [19]. The curve illustrates linear, nonlinear, and saturation regions relevant for traction and braking control.

Note: In this work, only longitudinal dynamics are considered. The Magic Formula parameters B_x , C_x , D_x , and E_x can be adapted according to normal load, vehicle speed, and tire properties to improve simulation fidelity.

3.3.1 Slip Ratio Definition

The longitudinal slip ratio σ is defined as:

$$\sigma = \frac{v_x - \omega R}{v_x} \tag{3.16}$$

where v_x is the longitudinal speed of the wheel hub, ω is the wheel angular velocity, and R is the effective tire radius. Positive σ corresponds to driving torque (acceleration), while negative σ indicates braking. For controlling traction and getting the best power distribution, it is important to get a good idea of σ .

3.3.2 Integration with Vehicle Dynamics

The Pacejka '96 tire model is combined with the quarter-car model to study how things interact with each other of the vehicle. The longitudinal tire force F_x , which is found in equation (3.13), affects the longitudinal motion of the sprung and unsprung masses, which can be seen in equations (3.10) and (3.4). At the same time, the vertical stiffness k_z and damping c_z of the tire are combined with the vertical suspension forces to effectively replicate tire-road interaction over various road surfaces. This connection enables the testing of slide control techniques and traction control systems (TCS) in electric vehicles equipped with motors in the wheels.

3.3.3 Illustrative Force-Slip Curve

Figure 3.4 illustrates a standard longitudinal force-slip curve produced by the Pacejka' 96 model. The initial linear region indicates small slip ratios, during which the tire force exhibits a nearly proportional increase with respect to slip. Tire force restrictions and possible loss of traction are shown by the curve's saturation beyond the peak. To make PID-based torque controllers and slip control algorithms that stop wheels from slipping too much and improve performance in the vehicle stability, it is important to understand its mathematical relation.

3.3.4 Applications in In-Wheel Motor Vehicles

The independent torque control at each wheel of an in-wheel motor electric car can provide us change F_x in real time based on the slip ratio σ . Using the Pacejka' 96 model with PID-based torque controllers offer us:

- Limit wheel slip to get the most traction on roads with different levels of friction,
- Coordinate longitudinal and vertical dynamics to reduce pitch and make the ride more comfortable,

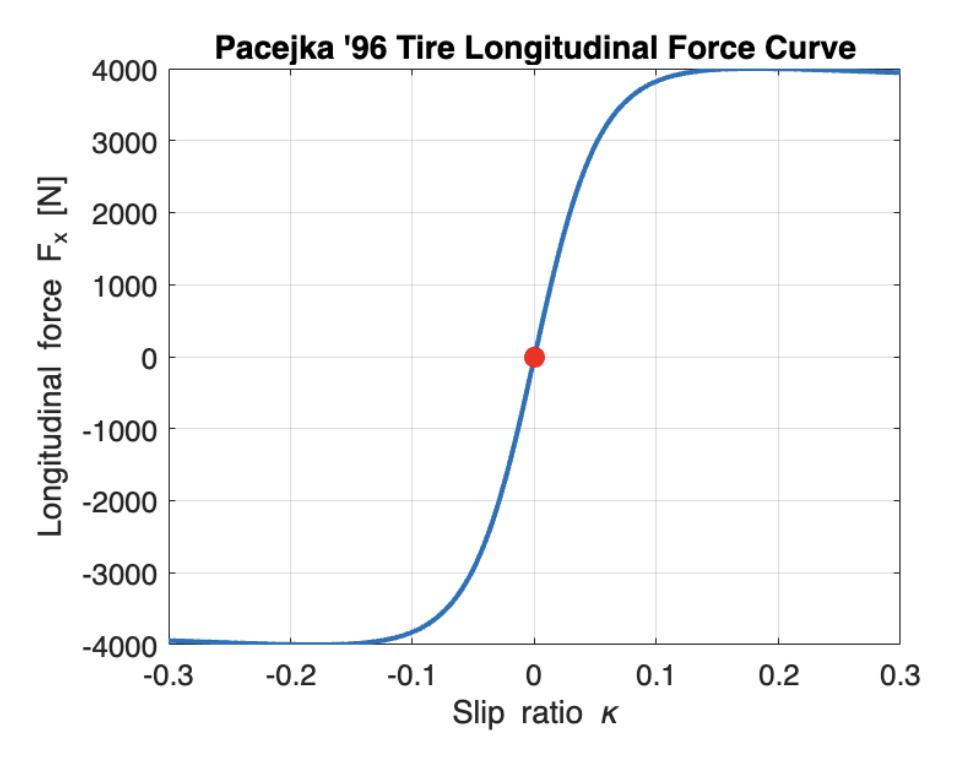


Figure 3.4: Illustration of the longitudinal tire force as a function of slip ratio based on the Pacejka '96 model [19]. The curve illustrates linear, nonlinear, and saturation regions relevant for traction and braking control.

- Simulate regenerative braking while keeping the wheels from locking up,
- Test how different suspension control strategies (Skyhook, Groundhook, Hybrid) affect the forces between the tires and the road.

This deeper integration shows how a physically realistic tire model, along with active suspension and advanced torque control strategies, can improve the comfort and handling of a car as a whole.

3.4 Road Profiles

For evaluating the performance of a vehicle's suspension, ride comfort, and tire-road interaction, it is important to accurately depict road irregularities. In this study, several road profiles are examined to evaluate the influence of extra unsprung mass and the effectiveness of active control systems.

3.4.1 ISO 8608 Class C Road

ISO 8608 [13] provides a uniform approach for categorizing road roughness by utilizing Power Spectral Density (PSD) to analyze surface irregularities. Roads are categorized

through a uniform system that encompasses different classifications. Class A represents exceptionally smooth highways, whereas Class H indicates extremely rugged off-road terrain. Classes C and D refer to somewhat rugged secondary paved roads that are typically utilized by passenger vehicles. Profilometers, accelerometers, or laser scanning techniques are used to get the measurements of how rough the road is. These measurements are critical for assessing suspension response, tire wear, and ride comfort.

For the simulations, the Class C road profiles is employed:

- A variable friction profile ranging 0–100 m was defined as follows:
 - $\mu = 0.8$ for the base road (0–50 m),
 - $\mu = 0.17$ in the region of the first bump (50–100 m),
- This setup was used to evaluate controller performance under multiple changes in traction conditions.

ISO 8608 Class C Road Profile Elevation (m) Coefficient H Coeffi Road Elevation Profile 0 20 60 40 80 100 Distance (m) Friction Coefficient Distribution 40 20 60 100 80 Distance (m) Zoomed-in Road Profile (72.1-82.1 m) 72 74 76 78 80 82 Distance (m)

Figure 3.5: ISO 8608 Class C road profile used in simulations.

3.4.2 Four Bumps Road Profile

A synthetic road profile with discrete bumps is also considered. The profile consists of four same bumps located at 20 m, 40 m, and 60 m along a 80 m stretch. The road-tire friction varies along the road, representing real-world conditions. For detailed analysis, a zoomed view of a single bump is extracted to examine suspension and tire response at localized irregularities.

• A variable friction profile ranging 0–100 m was defined as follows:

```
\mu = 0.8 for the base road (0–20 m, 30–40 m, 50–60 m),
```

 $\mu = 0.17$ in the region of the first bump (20–30 m), $\mu = 0.3$ in the region of the second bump (40–50 m), $\mu = 0.17$ for the third bump and the remaining road section ($x \ge 60$ m).

• This setup was used to evaluate longitudinal controller performance under multiple changes in traction conditions.

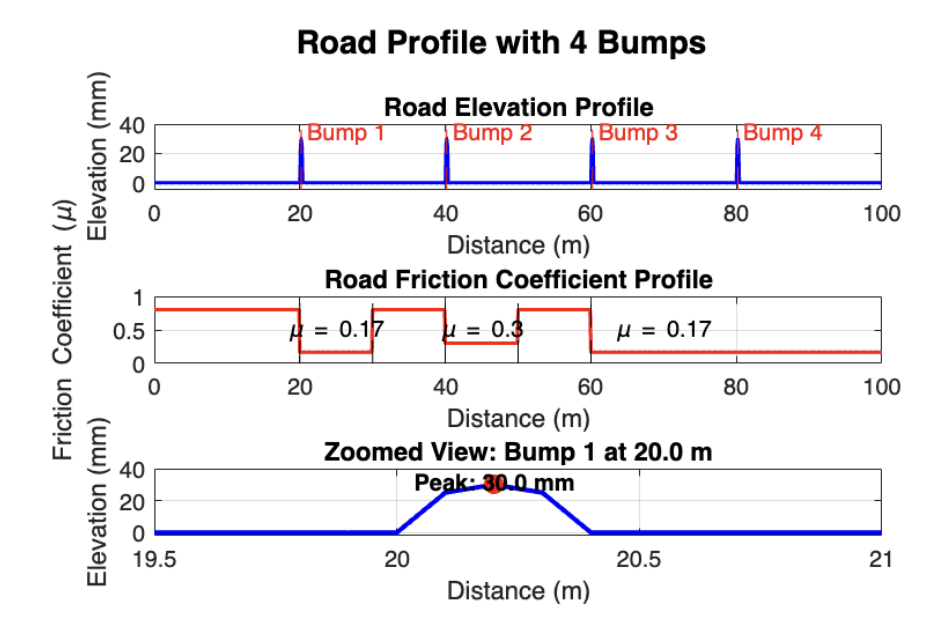


Figure 3.6: Four-bump road profile with varying friction.

3.5 Road Profile Enveloping Model and Simulation Scenarios

The generated road profiles are used to provide the inputs for the quarter-car model. While the original profiles define the vertical displacement z_r along the road, the quarter-car model requires inputs in terms of road elevation ω and road slope β . To bridge this, a road profile enveloping model is employed [12].

$$w(x_u) = \frac{Z_{e,fc} + Z_{e,rc}}{2} - b_c \tag{3.17}$$

$$\tan \beta_y(x_u) = \frac{Z_{e,fc} - Z_{e,rc}}{l_s} \tag{3.18}$$

where $Z_{e,fc}$ and $Z_{e,rc}$ are the vertical positions of the front and rear ellipse centers, b_c is the vertical semi-axis of the ellipse, and l_s is the longitudinal spacing between front and rear ellipses.

The front and rear ellipses are described by:

$$\left(\frac{x_{e,fc}}{a_c}\right)^c + \left(\frac{z_{e,fc}}{b_c}\right)^c = 1$$
(3.19)

$$\left(\frac{x_{e,rc}}{a_c}\right)^c + \left(\frac{z_{e,rc}}{b_c}\right)^c = 1 \tag{3.20}$$

where a_c and b_c are the horizontal and vertical semi-axes, and c is the ellipse shape parameter.

The effective height at the contact patch is obtained as the maximum vertical position along the ellipse:

$$Z_{e,fc} = \max \left(z_r(x_w, x_{e,fc}) + d_{fc}(x_{e,fc}) \right), \quad x_{e,fc} \in [-a_c, a_c]$$
 (3.21)

$$Z_{e,rc} = \max (z_r(x_w, x_{e,rc}) + d_{rc}(x_{e,rc})), \quad x_{e,rc} \in [-a_c, a_c]$$
 (3.22)

The distances from the ellipse centers to the bottom boundary are:

$$d_{fc}(x_{e,fc}) = b_c \left(1 - \left|\frac{x_{e,fc}}{a_c}\right|^c\right)^{1/c} \tag{3.23}$$

$$d_{rc}(x_{e,rc}) = b_c \left(1 - \left|\frac{x_{e,rc}}{a_c}\right|^c\right)^{1/c} \tag{3.24}$$

This method ensures a smooth, continuous representation of road irregularities that properly accounts for vehicle geometry, enabling more accurate simulation of suspension and tire dynamics under realistic road conditions.

3.6 Controllers Design

A longitudinal slip controller and a vertical active suspension controller are used in this work to improve the performance of the car. The longitudinal controller uses a PID method to control tire slip by changing the torque, and the vertical controller uses a active approach (Skyhook, Groundhook, Hybrid) to make the ride more comfortable and improve handling.

3.6.1 Longitudinal Slip Controller

This longitudinal control technique tries to keep the wheel slip σ close to a certain number σ_{ref} so that the vehicle can stop and grip better. Inputting the current unsprung mass state (m_u) finds the reference slip using a look-up table that already exists and displays the optimal slip for different road conditions and tire characteristics. The control law then computes the slip error:

$$e_{\sigma} = \sigma_{\text{ref}} - \sigma_{\text{act}} \tag{3.25}$$

This error is processed through a PID controller to generate a torque correction ΔT_m :

$$\Delta T_m(s) = \frac{200s^2 + 200s + 100}{s^2 + s} E_{\kappa}(s)$$
 (3.26)

where $E_{\kappa}(s)$ is the Laplace transform of the slip error. The root locus method, a graphical technique for evaluating the movement of the closed-loop poles of the system with varying gains, was employed to adjust the PID parameters. The introduction of zeros in the PID controller results in a leftward shift of the poles in the complex plane, which enhances stability and accelerates the response time. In the interim, supplementary poles are employed to filter high-frequency components, thereby reducing oscillations. The PID gains were changed over and over by looking at the root locus to find the best mix between quick slip correction and strong stability.

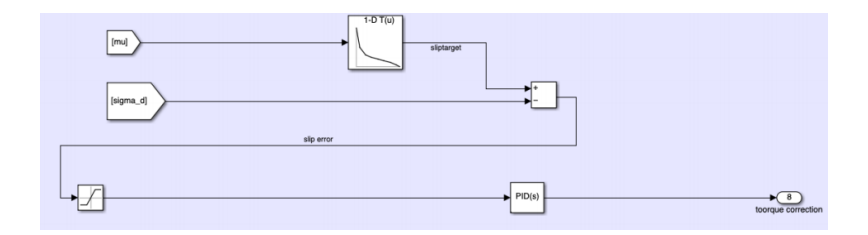


Figure 3.7: Schematic of the longitudinal slip control loop implemented in Simulink.

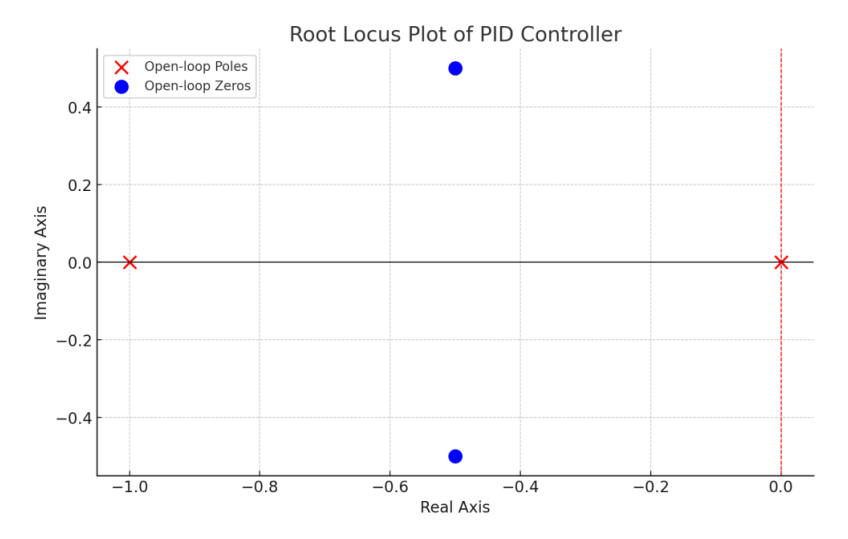


Figure 3.8: Root locus of the longitudinal PID controller showing closed-loop pole trajectories.

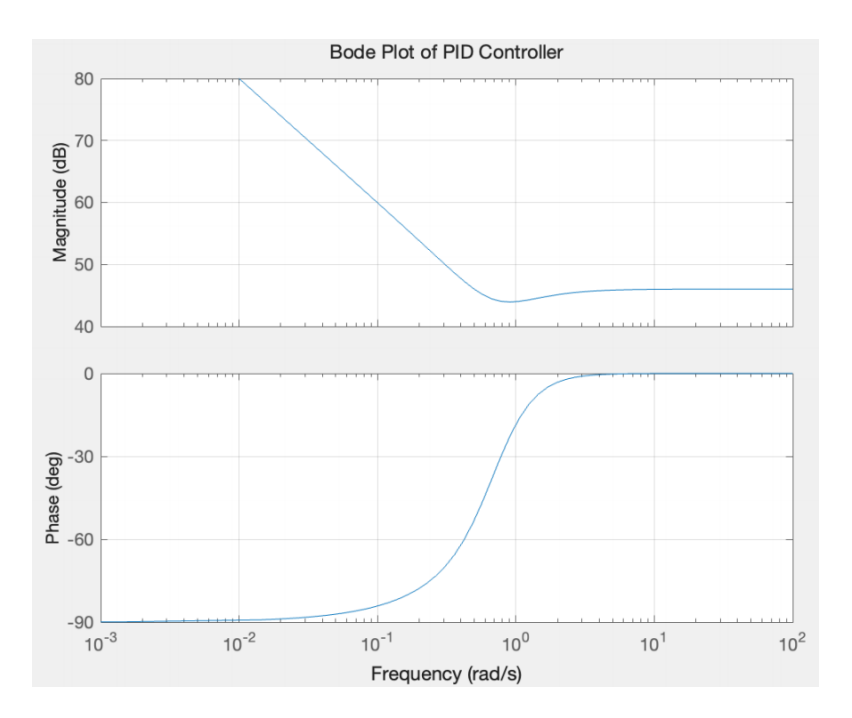


Figure 3.9: Bode plot of the PID controller demonstrating frequency response characteristics.

3.6.2 Vertical Active Controllers: Skyhook, Groundhook, and Hybrid

The goal of vertical active control methods is to adjust the controlling force of the suspension to enhance the ride comfort and the car handling.

Skyhook Control

Skyhook control targets the reduction of vehicle body oscillations by simulating a virtual damper between the sprung mass and an inertial reference (the "sky"):

$$F_{\rm sky} = c_s \, \dot{z}_s \tag{3.27}$$

where:

- c_s is the damping coefficient of the skyhook controller,
- \dot{z}_s is the vertical velocity of the sprung mass.

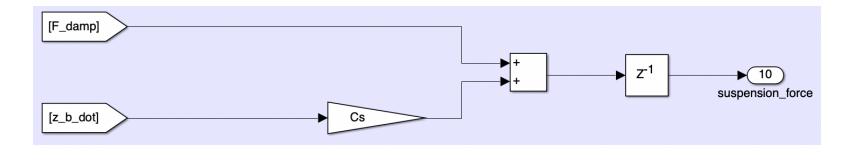


Figure 3.10: Block diagram of active Skyhook controller.

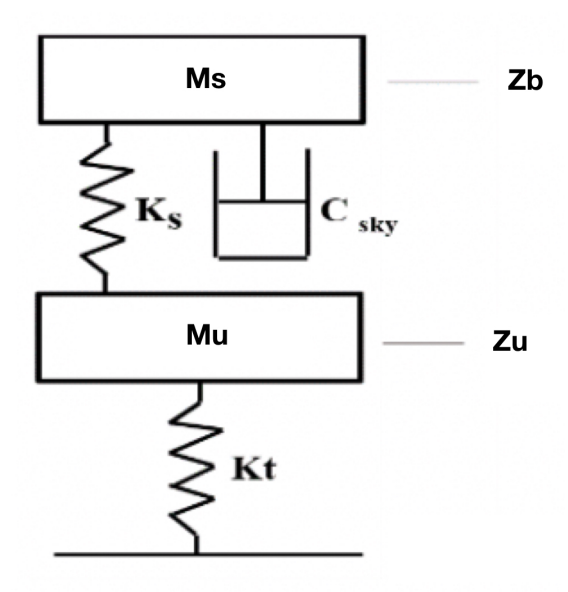


Figure 3.11: schematic of active Skyhook controller.

Groundhook Control

Groundhook control focuses on improving road-holding performance by damping unsprung mass oscillations. It simulates a actuator between the unsprung mass and the road surface:

$$F_{\text{ground}} = c_g \, \dot{z}_u \tag{3.28}$$

where:

- c_q is the damping coefficient of the groundhook controller,
- \dot{z}_u is the vertical velocity of the unsprung mass.

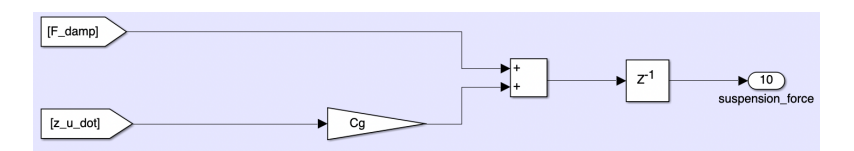


Figure 3.12: Block diagram of active Groundhook controller.

Hybrid Control

Skyhook and Groundhook logic are combined in hybrid control to find the best mix between ride comfort and road holding. The reducing force that is created is the weighted sum of the two methods that were used. The damper coefficient is adjusted based on a blending factor α that determines the relative influence of each control rule:

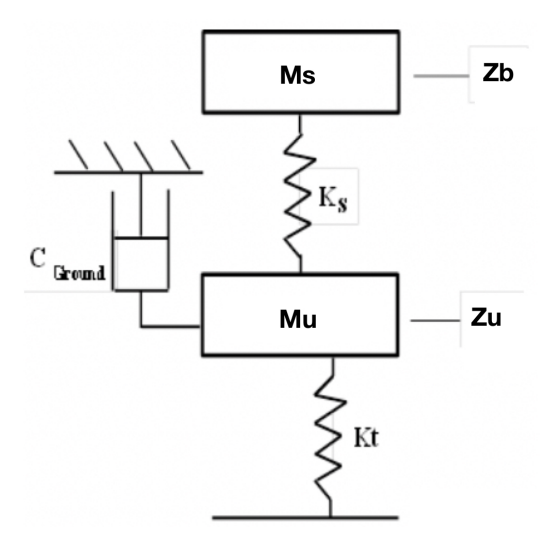


Figure 3.13: schematic of active Groundhook controller.

$$F_{\text{hybrid}} = \alpha c_s \dot{z}_s + (1 - \alpha) c_q \dot{z}_u \tag{3.29}$$

where:

- α is the weighting factor between skyhook and groundhook control $(0 \le \alpha \le 1)$,
- c_s is the damping coefficient of the skyhook controller,
- c_g is the damping coefficient of the groundhook controller,
- \dot{z}_s and \dot{z}_u are the vertical velocities of the sprung and unsprung masses, respectively.

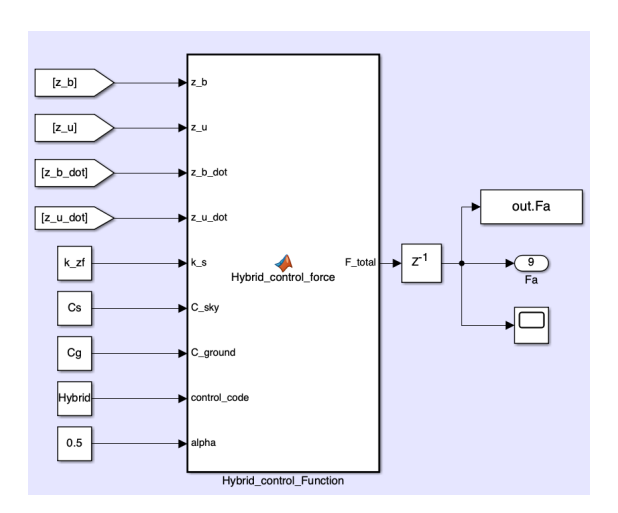


Figure 3.14: Block diagram of active Hybrid controller combining Skyhook and Groundhook logic.

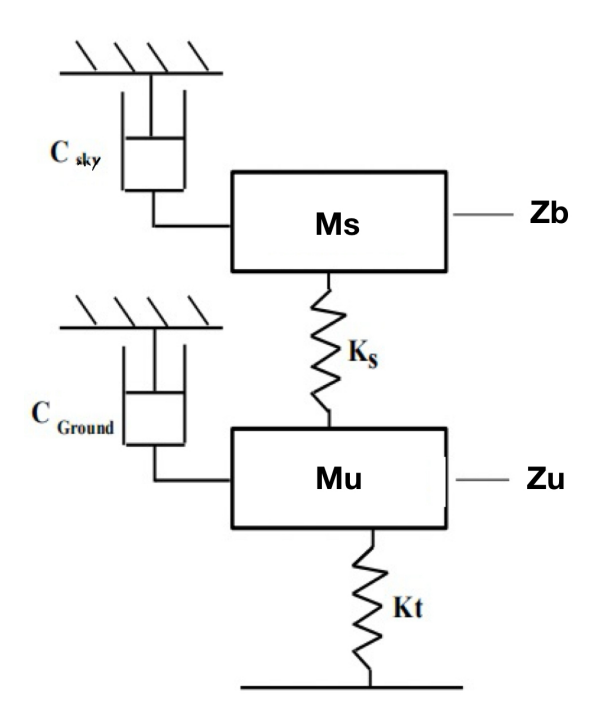


Figure 3.15: schematic of active Hybrid controller.

The active suspension system can change the active force dynamically in response to changes in the road and the way the car moves by the vertical control strategies. The Skyhook is more focused on comfort, the Groundhook is more focused on road holding, and the Hybrid is a compromise for the balance between passenger comfort and road holding performance for in-wheel motor cars with more unsprung mass.

3.7 Key Performance Indicators (KPIs)

Several key performance indicators (KPIs) are set up so that car performance can be systematically evaluated in a range of road and control situations. These KPIs check how smooth the ride is, how well the car can grip the road, how much traction it has, and how well it can keep from slipping.

3.7.1 Sprung-Mass Weighted Vertical Acceleration

Measurements of the sprung mass's vertical acceleration are used to judge the comfort of the ride. ISO 2631 [14] describes standard ways to measure how people react to whole-body vibrations by using frequency-dependent weighting functions on raw acceleration data. The weighted vertical acceleration highlights the frequencies that are most noticeable to human occupants:

$$a_w = W(f) \cdot a \tag{3.30}$$

where:

- a_w is the weighted vertical acceleration (m/s²),
- a represents the raw vertical acceleration of the sprung mass (m/s^2) ,
- W(f) is the ISO 2631 frequency weighting function [9].

As seen from the point of view of vertical dynamics, the root-mean-square (RMS) of the body acceleration is:

$$a_{w,\text{rms}} = \sqrt{\frac{1}{T} \int_0^T (a_w(t))^2 dt},$$
 (3.31)

where $a_w(t)$ is the vertical acceleration of the sprung mass over the observation interval T. The weighting function prioritizes the frequency range of 0.5–80 Hz, which corresponds to human sensitivity to vibration [10]. Lower a_w corresponds to improved ride comfort.

3.7.2 Road-Holding Index (RHI)

Road-holding capability is quantified via the Road Holding Index (RHI), which evaluates the suspension's ability to maintain tire-road contact [17, 12]:

$$RHI = \frac{k_{tf} \cdot (z_u - w)}{m \cdot g} \tag{3.32}$$

where:

- k_{tf} is the vertical tire stiffness (N/m),
- z_u is the vertical displacement of the unsprung mass (m),
- w is the road surface displacement (m),
- m is total vehicle mass (kg),
- g is gravitational acceleration (9.81 m/s²) [20].

A lower RHI indicates more consistent tire-road contact and improved stability.

3.7.3 Maximum Tire Slip

Traction is measured by the maximum slip ratio λ , which can be found by [19, 3]:

$$\lambda = \frac{V_w - V_x}{V_x} \times 100\% \tag{3.33}$$

where V_w is wheel tangential velocity and V_x is longitudinal vehicle velocity. Maximum slip is critical for evaluating traction, stability, and braking performance.

3.7.4 Slip Error Integral

The cumulative deviation of actual tire slip from the desired slip is captured by the slip error integral [10]:

$$I_{\text{slip}} = \int_0^T (\lambda_{\text{desired}} - \lambda_{\text{actual}}) dt$$
 (3.34)

Lower $I_{\rm slip}$ values indicate effective slip control, improved traction, and vehicle stability under varying road conditions.

3.7.5 Summary of KPIs

Table 3.4 summarizes the defined KPIs:

Table 3.4: Key Performance Indicators for Vehicle Evaluation

KPI	Definition	Unit / Note
Weighted Acceleration	$a_w = W(f) \cdot a$	m/s^2 , ISO 2631 weighted
Road-Holding Index	$RHI = k_{tf}(z_u - w)/(mg)$	Dimensionless
Maximum Slip	$\lambda = (V_w - V_x)/V_x \cdot 100\%$	%
Slip Error Integral	$I_{\text{slip}} = \int_0^T (\lambda_{\text{desired}} - \lambda_{\text{actual}}) dt$	Dimensionless

3.8 Vehicle Parameters

The main physical parameters used in the quarter-car model are listed in Table 3.5.

Table 3.5: Vehicle parameters used in the simulation

Parameter	Symbol	Value
Sprung mass	m_s	564 kg
Unsprung mass	m_u	79 kg
Suspension stiffness	k_s	25,500 N/m
Tire stiffness	k_t	381,914 N/m

The resonance frequencies of the sprung and unsprung masses, often referred to as the body and wheel resonance frequencies, are expressed as follows:

$$f_{\text{body}} = \frac{1}{2\pi} \sqrt{\frac{k_s}{m_s}} \tag{3.35}$$

$$f_{\text{wheel}} = \frac{1}{2\pi} \sqrt{\frac{k_t + k_s}{m_u}} \tag{3.36}$$

The body and wheel resonance frequencies are 1.07 Hz and 11.42 Hz respectively.

Chapter 4

Results and Discussion

4.1 ISO 8608 Class C Road with Constant Friction Coefficient (μ)

This type of road is used for studying how the extra unsprung mass will impact the KPIs for the vehicle's dynamics performance. Small and larger unsprung were tested under ISO road with Skyhook+TCS.

Table: Influence of In-Wheel Motor (IWM) on Performance

Donomoton	Big Unsprung Mass	Small Unsprung Mass	
Parameter	$(\mathrm{IWM} + 24 \mathrm{\ kg})$	(No~IWM)	
$a_{w,\text{rms}} (\text{m/s}^2)$	3.908×10^{-1}	3.839×10^{-1}	
$\mathrm{RHI}_{\mathrm{rms}}$	1.010×10^{-3}	9.560×10^{-4}	
$\sigma_{ m max}$	1.978×10^{-2}	1.535×10^{-2}	
$I_{ m slip}$	4.540×10^{-2}	3.810×10^{-2}	

4.1.1 Comfort Analysis

With a bigger unsprung mass, the vertical acceleration is a little higher (0.38398 \rightarrow 0.39082 m/s²), going up by about 1.75%. This means that when the unsprung mass is bigger, the passenger feels more bumps in the road. It is harder for the wheel to follow the road when the unsprung mass is higher. This makes the suspension work harder, which makes the ride rougher. In short, more unsprung mass makes the ride less comfortable by letting people feel more of the road's movements. Getting rid of unsprung mass makes the ride better by letting the wheels move more smoothly over rough ground.

4.1.2 Handling Performance

When the unsprung mass is higher $(0.000956 \rightarrow 0.001010)$, the road holding index goes up by 5.35%. This is clear from Fig. 4.3, which shows that wheels move more when the unsprung mass is greater. A heavier unsprung mass makes it harder for the tire to keep a steady touch with the road because the tire force changes more frequently.

4.1.3 Stability and Slip Control

When the unsprung mass is bigger $(0.0381 \rightarrow 0.0454)$, the slip error goes up by 16.08%, while the maximum slip $(0.01535 \rightarrow 0.01978)$ goes up by 28.87%. Slip changes are also much less regular when the unsprung mass is bigger, as the high-frequency spikes in the blue graph show. When slow down or speed up, it is harder to control slip with a unsprung mass which is larger. When a wheel has larger inertia, it takes longer to adjust to sudden changes in speed, which makes slip variations bigger. The instability makes it harder for traction control devices to keep the grip. Slip movements that get worse also make ABS and traction control systems less useful.

4.1.4 Implications for Control Strategies

A larger unsprung mass influences the physics of both the longitudinal (traction) and vertical (comfort and stability) directions. It is important to use advanced control techniques because the extra weight makes it harder for the wheels to stay on the road. Traction Control Systems (TCS) help by adjusting the torque to reduce slip, but this is not enough to fully stabilize the car. For maintaining stability on uneven surfaces and minimizing unnecessary motions, vertical control systems such as active suspension systems are essential. Using TCS with adaptive suspension gives more control over both the movement of the vehicle and the comfort of the ride at the same time. This makes sure that the vehicle works better in all kinds of driving situations and stays stable when speeding up, slowing down, or cornering.

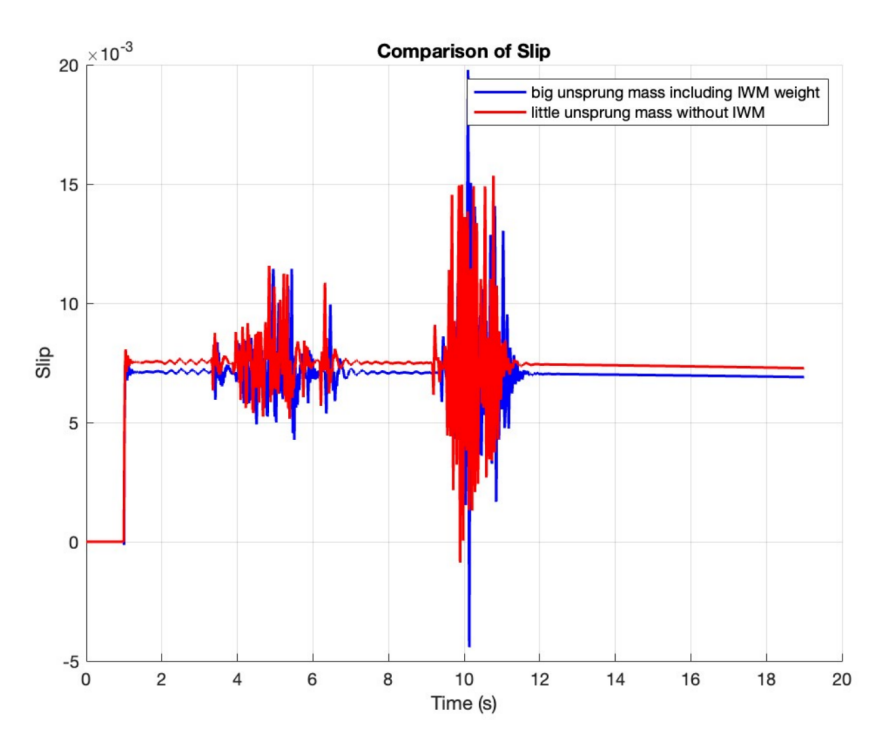


Figure 4.1: Comparison of slip with and without IWM

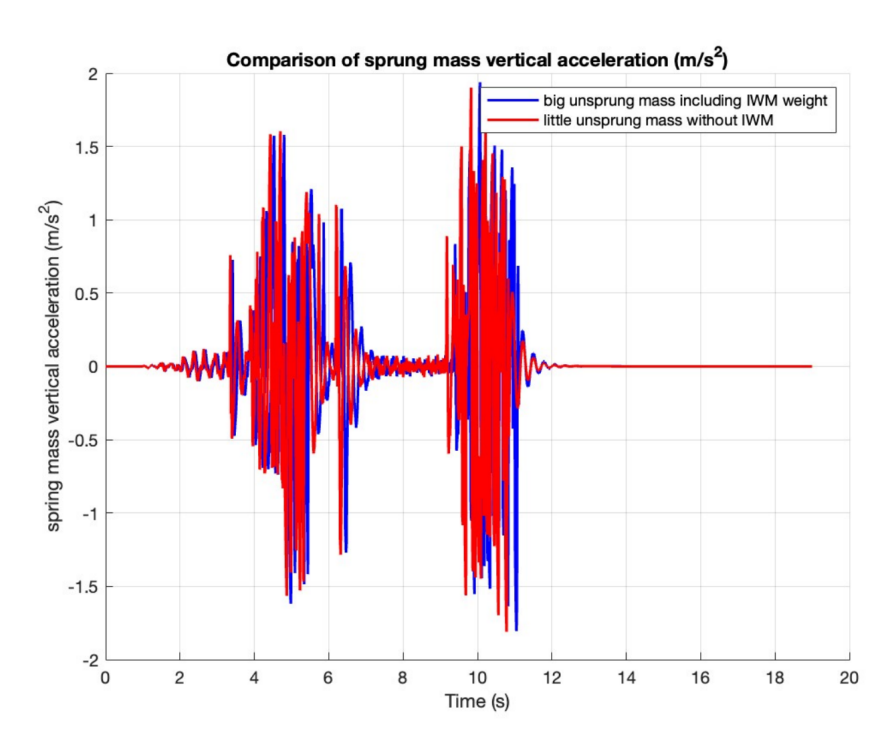


Figure 4.2: Comparison of sprung mass vertical acceleration with and without IWM

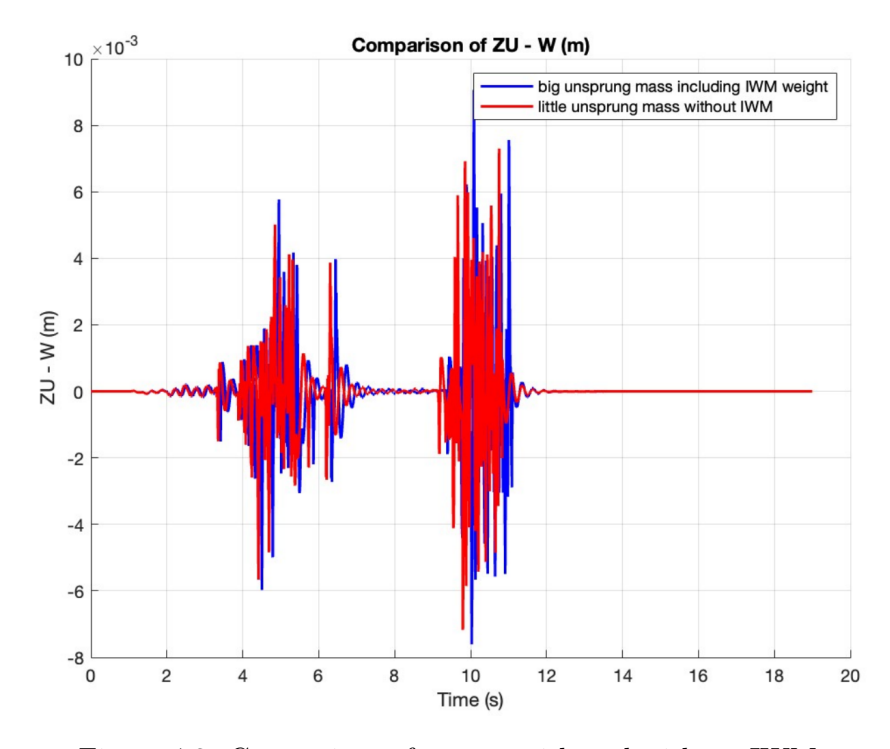


Figure 4.3: Comparison of z_u-w with and without IWM

Larger unsprung mass due to extra weight of IWM, as shown in the figures, this makes

all the performance indicators worse.

4.2 ISO 8608 Class C Road with Variable Friction Coefficient (μ)

This road profile is used to see the effect of the suggested controllers work and how they affect the performance of vehicle. A performance investigation was performed on a 100 m ISO Class C road exhibiting a variable friction coefficient (μ). Four configurations were tested:

- Uncontrolled (Passive Damper),
- Skyhook + TCS,
- Groundhook + TCS,
- Hybrid + TCS.

These Key Performance Indicators (KPIs) were looked at:

- $a_{w,\text{rms}}$ (m/s²): Checks how comfortable the ride is. When values are lower, comfort is higher.
- RHI_{rms}: Checks how well the handling works. Lower values mean that the tires have better touch with the road.
- σ_{max} : The highest value of slip. It is better to have lower numbers for traction and stability.
- $I_{\rm slip}$: This measure adds up the slip error. Lower values are preferable.

Table 4.1 shows a summary of the results, and the main findings are as follows:

- Skyhook + TCS method lowers the RMS of body acceleration by a large amount, which makes the ride more comfortable.
- Groundhook + TCS makes the tires touch the road better, which makes the road holding performance better.
- TCS effectively stops excessive slip, lowering σ_{max} and I_{slip} compared to the scenario where there is no control.
- The Hybrid + TCS provides a balance in efficiency because it reduces both vibration and slip.

Table 4.1 shows the KPI values that were found when the road was excited to ISO Class C, which means that the random broadband profile caused constant vibration. The review takes into account the 24 kg of extra unsprung mass that comes from IWMs.

Table 4.2 shows the energy consumption KPIs that were found under the same ISO Class C road excitation, which provides a constant random broadband vibration. These values represent the energy consumed by the active damper under each control logic, with the Passive strategy serving as a zero-comsumption reference.

Table 4.1: Influence of Increased Unsprung Mass on Vehicle Performance (ISO Class C Road, Variable μ)

KPI	Control Strategy			
	Passive	Skyhook+TCS	Groundhook+TCS	Hybrid+TCS
$a_{w,\mathrm{rms}}~(\mathrm{m/s^2})\downarrow$	0.45364	0.11682	0.25117	0.17594
$\mathrm{RHI}_{\mathrm{rms}}\downarrow$	0.015401	0.031613	0.013349	0.014379
$\sigma_{ m max}\downarrow$	0.88813	0.019505	0.012999	0.01243
$I_{ m slip}\downarrow$	9.1774	0.024032	0.019366	0.019641

Table 4.2: Energy Consumption Comparison (ISO Class C Road, Variable μ)

KPI	Control Strategy			
	Passive	Skyhook	Groundhook	Hybrid
Energy Consumption (J/km)	0	981.0	429.8	898.0
Average Power (W)	0	4.91	2.15	4.49

4.2.1 Ride Comfort Analysis

The random road excitation generates continuous vibrations that strongly affect ride comfort. In the passive case, the weighted RMS acceleration is 0.45364 m/s^2 . Skyhook+TCS reduces this value drastically to 0.11682, corresponding to an improvement of nearly 74.3%. Groundhook+TCS (0.25117) and Hybrid+TCS (0.17594) also attenuate vibrations compared to Passive with reduction by 44.6% and 61.22%, but less effectively than Skyhook. This confirms the advantage of Skyhook damping in mitigating sustained low-frequency body vibrations on ISO road profiles [6].

4.2.2 Handling Performance

The Road Holding Index reduces from 0.015401 (Passive) to 0.031613 (Skyhook+TCS), 0.013349 (Groundhook+TCS), and 0.014379 (Hybrid+TCS). While all active strategies improve contact quality, Groundhook+TCS provides the lowest RHI with reduction over 13.3%, suggesting the most stable tire—road contact. Hybrid, although slightly higher in RHI than Ground, achieves a good balance between comfort and handling.

4.2.3 Stability and Slip Control

Without TCS control, the ISO profile causes excessive slip, with $\sigma_{\rm max}=0.88813$ and $I_{\rm slip}=9.1774$. Skyhook+TCS reduces these values dramatically to $\sigma_{\rm max}=0.019505$ and $I_{\rm slip}=0.024032$, suppressing both peak and accumulated slip oscillations. Groundhook+TCS (0.012999, 0.019366) and Hybrid+TCS (0.01243, 0.019641) also improve stability but remain less effective than Skyhook. While all the strategies with TCS can provide reduction over 95% means PID controller works properly. This demonstrates

that under broadband disturbances, the slip amplification due to IWMs can be efficiently counteracted by longitudinal PID-based integrated control [8, 21].

4.2.4 Implications for Control Strategy Selection

In the context of ISO road excitation, the Skyhook+TCS system demonstrates substantial overall enhancements. It achieves a reduction in RMS acceleration by nearly an order of magnitude, decreases slip ratios by over 95%, and maintains stable tire—road contact. Hybrid+TCS delivers optimal RHI performance; however, it compromises a degree of comfort in comparison to Skyhook. Groundhook+TCS presents the least advantageous choice, providing only limited benefits. Therefore, Hybrid+TCS is a good way to combine strategies for finding a balance for vertical and longitudinal performance with more unsprung mass on bumpy roads.

4.2.5 Frequency Domain Response Analysis

Frequency-domain analysis (Fig. 4.7) provides critical insights into the control strategies' performance. The plot confirms that the ISO road's energy is concentrated in the 0.5–2 Hz band, the primary source of discomfort evident in the passive system's high PSD [16]. Skyhook+TCS demonstrates exceptional effectiveness by significantly reducing PSD within this essential range, thereby confirming its outstanding comfort metric. On the other hand, Groundhook+TCS only suppress gain in these frequencies range a little, which makes sense as it focuses on suppressing higher-frequency wheel hop. The Hybrid strategy's PSD curve is in the middle of the two, which shows that it strikes a good compromise between comfort and road-holding.

4.2.6 Energy Consumption for Control Strategy Selection

Under ISO Class C excitation, the **Skyhook+TCS** strategy shows the highest energy consumption (981 J/km, 4.9 W), reflecting its active suppression of body motion and improved comfort at the expense of efficiency. The **Groundhook+TCS** strategy achieves the lowest energy use (430 J/km, 2.15 W), prioritizing tire–road contact with minimal actuator effort but reduced comfort. The **Hybrid+TCS** strategy (898 J/km, 4.49 W) provides a balanced trade-off, offering near-Groundhook stability with lower energy demand than Skyhook, making it the most practical and efficient choice overall.

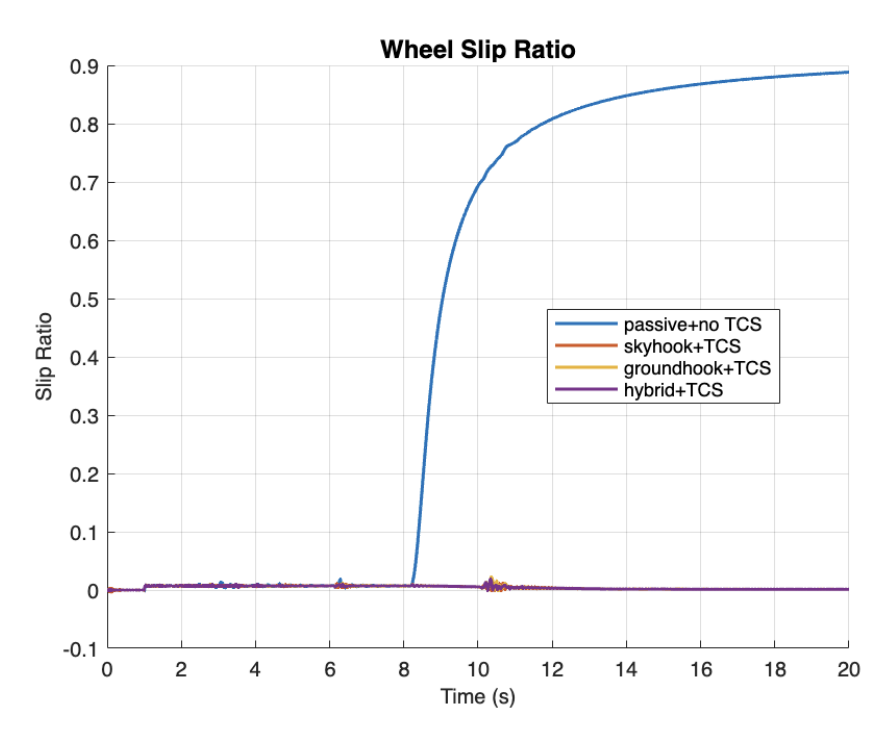


Figure 4.4: ISO road – Wheel Slip Ratio

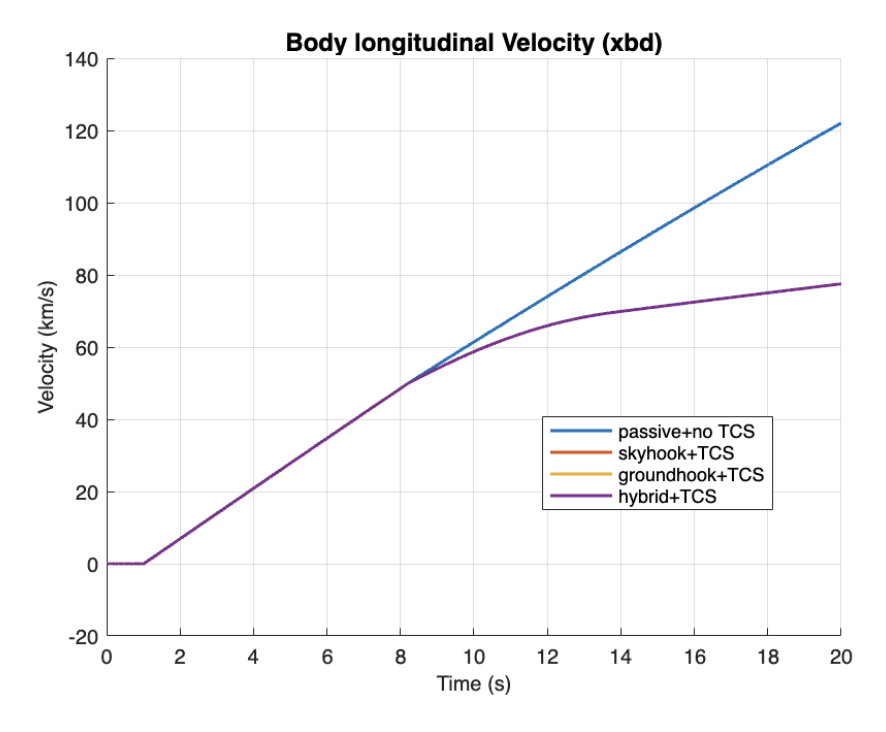


Figure 4.5: ISO road – Body Longitudinal Velocity (x_{bd})

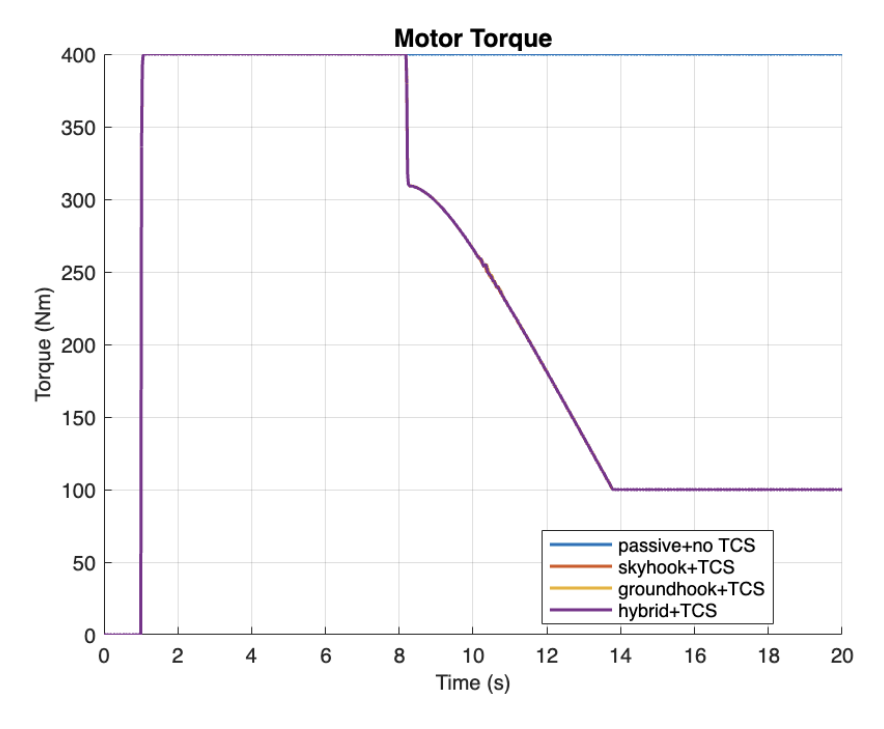


Figure 4.6: ISO road – Motor Torque

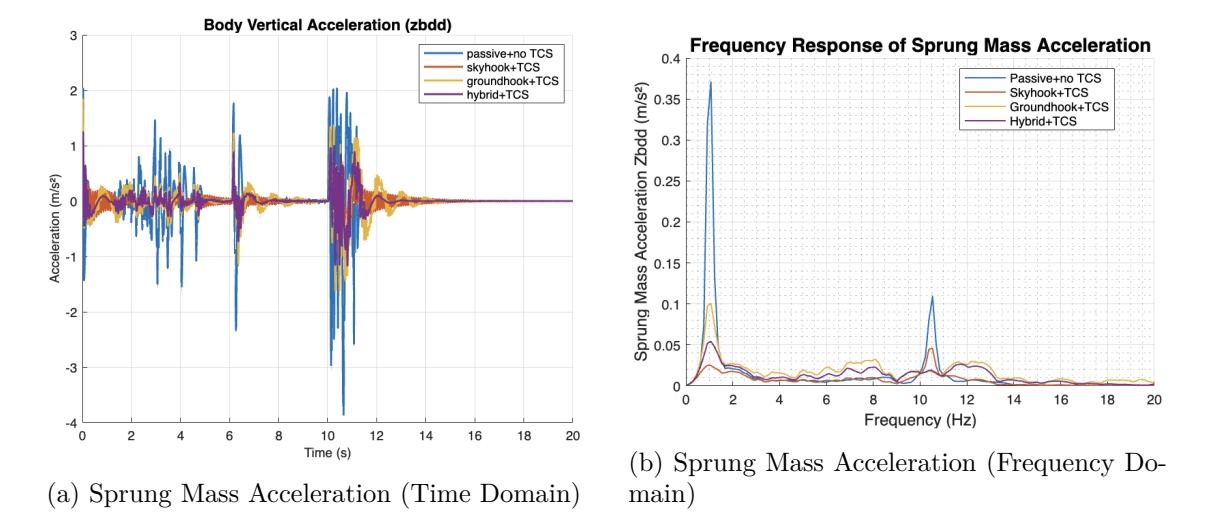


Figure 4.7: ISO road – Sprung Mass Acceleration responses.

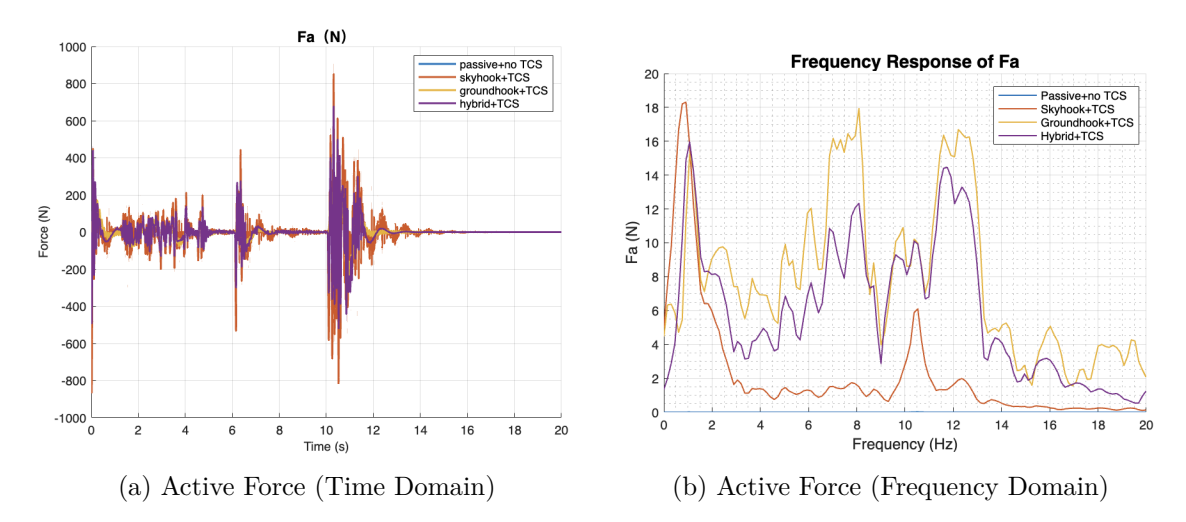


Figure 4.8: ISO road – Active Force responses.

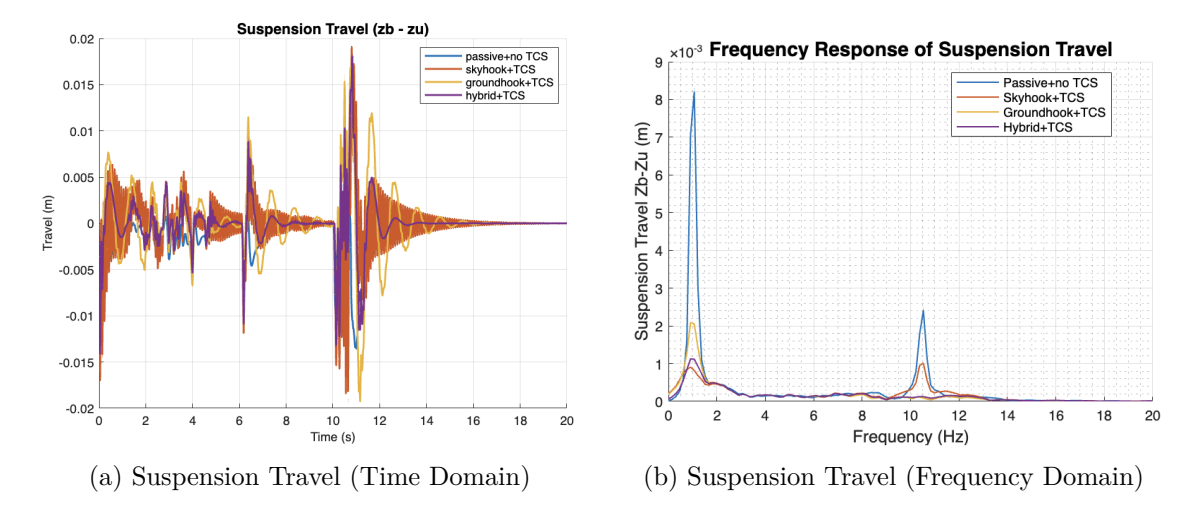
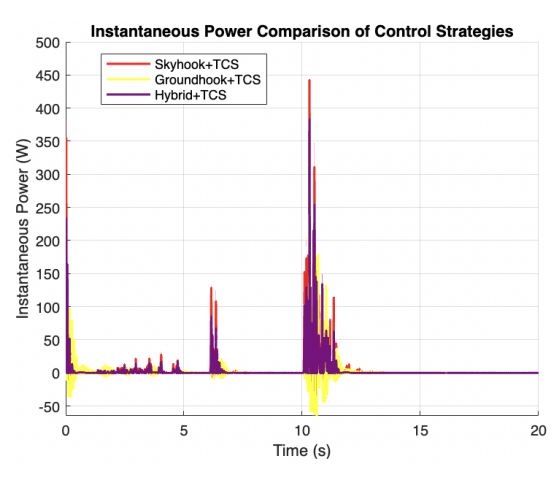
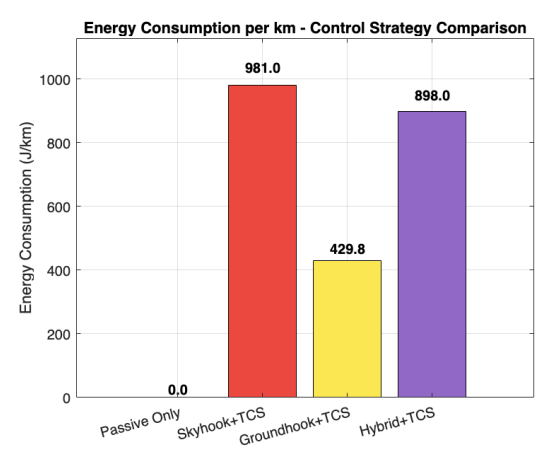


Figure 4.9: ISO road – Suspension Travel responses.





- (a) Instantaneous Power of Control Strategies
- (b) Cumulative Energy Consumption Comparison

Figure 4.10: ISO road – Power and Energy Consumption.

Under ISO Class C excitation, Skyhook + TCS achieves the best ride comfort but with the highest energy demand. Groundhook + TCS minimizes tire load and power use, while Hybrid + TCS provides a balanced trade-off between comfort, road holding, and efficiency. The highest frequency response peak can be found at body resonance frequency range around 1 Hz.

4.3 Four Bumps Road with Variable Friction Coefficient (μ)

This road profile is defined as a 100 m track containing four equally spaced bumps positioned at 20 m, 40 m, 60 m, and 80 m. The road friction coefficient (μ) varies along the distance, allowing for the assessment of controller robustness under changing grip conditions. The objective is to evaluate the effectiveness and influence of the controllers.

Four strategies were tested:

- Uncontrolled (Passive Damper)
- With Two Controllers (Skyhook + TCS)
- With Two Controllers (Groundhook + TCS)
- With Two Controllers (Hybrid + TCS)

The following Key Performance Indicators (KPIs) were analyzed:

- $a_{w,P2P}$ (m/s²): Measures ride comfort. It is more comfortable when the values are lower.
- RHI_{P2P}: Checks how well dealing works. Lower values mean that the tires have better contact with the road.

- σ_{max} : Finds the highest value of slip. It is better to have lower numbers for traction and stability.
- $I_{\rm slip}$: Finds the total amount of slip mistake. It is better to have lower numbers.

Table 4.3 shows how well the different control methods worked when the four-bump road profile caused a transient disturbance, taking into account the extra 24 kg of unsprung mass caused by IWMs. These four KPIs, which are explained in Section 3.7, are used to do the review.

Table 4.3: Influence of Increased Unsprung Mass on Vehicle Performance (Four Bumps Road, Variable μ)

KPI	Control Strategy			
	Passive	Skyhook+TCS	Groundhook+TCS	Hybrid+TCS
$a_{w,\text{P2P}} (\text{m/s}^2) \downarrow$	10.5	4.3511	10.142	6.9644
$\mathrm{RHI}_{\mathrm{P2P}}\downarrow$	0.87547	1.4879	0.81969	0.84342
$\sigma_{ m max}\downarrow$	0.88347	0.32534	0.56193	0.47592
$I_{ ext{slip}}\downarrow$	9.0996	0.42579	0.3841	0.29794

Table 4.4 shows the energy consumption of the four identical bumps over a 100-meter distance. These values represent the energy consumed by the active actuators under each control logic. Notably, the Skyhook strategy becomes the most energy-intensive, while the Groundhook strategy remains the least energy-intensive.

Table 4.4: Energy Consumption Comparison (3cm Bumps Road)

KPI	Control Strategy			
	Passive	Skyhook	Groundhook	Hybrid
Energy Dissipation $(J/km) \downarrow$	0	7938	6005.9	7236.6
Average Power (W) \downarrow	0	39.69	30.03	36.18

4.3.1 Ride Comfort Analysis

The comfort metric $a_{w,P2P}$ shows that the four bumps induce severe body acceleration in the passive configuration (10.5 m/s²). When Skyhook control is applied with TCS, this value drops drastically to 4.3511, an improvement of nearly 58.6%. Conversely, Groundhook+TCS amplifies vertical vibrations (10.142) with reduction 3.4%, while Hybrid+TCS achieves only a partial reduction (6.9644) with reduction 33.7%. According to these results, Skyhook damping is the best way to stop sudden changes in excitement by attenuating the acceleration of sprung mass [6].

4.3.2 Handling Performance

The Road Holding Index indicates how well the wheels maintain contact during the bump sequence. Groundhook+TCS improves RHI_{P2P} from 0.87547 to 0.81969 with reduction 6.4%, suggesting better tire-road contact. Hybrid+TCS stays almost same performance (0.84342)with reduction around 3.7%. This outcome demonstrates that under transient inputs, Hybrid improves both comfort and road holding, while Groundhook prioritizes unsprung dynamics to increase road handling performance at the expense of overall vehicle stability [1].

4.3.3 Stability and Slip Control

Without controllers, the bump excitation generates excessive slip, with $\sigma_{\rm max} = 0.88347$ and $I_{\rm slip} = 9.0996$. Skyhook+TCS dramatically reduces slip to $\sigma_{\rm max} = 0.32534$ and $I_{\rm slip} = 0.42579$, indicating a suppression of both peak and accumulated slip oscillations. Groundhook+TCS and Hybrid+TCS also make the vehicle stable ($\sigma_{\rm max} = 0.56193$, 0.47592 and $I_{\rm slip} = 0.3841$, 0.29795), but not too much. It is clear from these data that the extra weight added by IWMs makes slip worse on uneven roads, but Skyhook control combined with TCS is the best at reducing it.

4.3.4 Implications for Control Strategy Selection

For the four bumps profile, Hybrid+TCS is definitely the best compromise. It keeps body acceleration to a lower value, improves road holding, and suppresses slippage. While Skyhook+TCS gives you better ride comfort but not perfect total performance, ground-hook+TCS makes passenger feel very uncomfortable even though it partly stabilizes wheel dynamics. So, even when there are temporary problems with the road, an integrated Hybrid-based approach is still the best way to handle vehicles that have additional unsprung mass with motors inside the wheels.

4.3.5 Frequency Domain Response Analysis

The frequency-domain response to the four-bump excitation, as shown in Fig. 4.14, clearly highlights the fundamental balance between comfort and road-holding. In contrast to the stochastic ISO road, these temporary effects produce a wide energy spectrum, significantly stimulating high-frequency wheel-hop resonance (8-12 Hz) vital for tire contact[16]. The Skyhook+TCS technique shows overall good performance by effectively lowering body resonance peaks. This clearly explains why it does a better job of lowering peak-to-peak body acceleration. The Groundhook+TCS method, on the other hand, does a great job by reducing the high-frequency wheel-hop peak but the low-frequency body resonance gain is high. This explains why its comfort score is low. The Hybrid+TCS strategy's PSD curve shows its compromise by giving balanced, attenuation at both important frequencies.

4.3.6 Energy Consumption for Control Strategy Selection

For the transient impulse-like excitation of the discreet bumps road, the trade-offs are similar. The $\mathbf{Skyhook+TCS}$ strategy, while offering the highest energy consumption (Table 4.2), demonstrates a significant compromise in passenger comfort, resulting in the worst road holding ($\mathbf{RHI_{rms}}$) and highest slippage (I_{slip}) as shown in Table 4.1. Conversely, the $\mathbf{Groundhook+TCS}$ strategy delivers the best road holding and slip suppression. However, this superior grip comes at the cost of the lowest energy consumption and is widely known to degrade passenger comfort by increasing body acceleration. Therefore, the $\mathbf{Hybrid+TCS}$ strategy presents the most balanced and robust solution for this common driving scenario. It achieves road holding and slip performance nearly identical to the Groundhook strategy, but does so with lower energy consumption and implies a much better comfort trade-off. This suggests the integrated Hybrid-based approach is the most practical and efficient solution for daily driving in IWM-equipped vehicles.

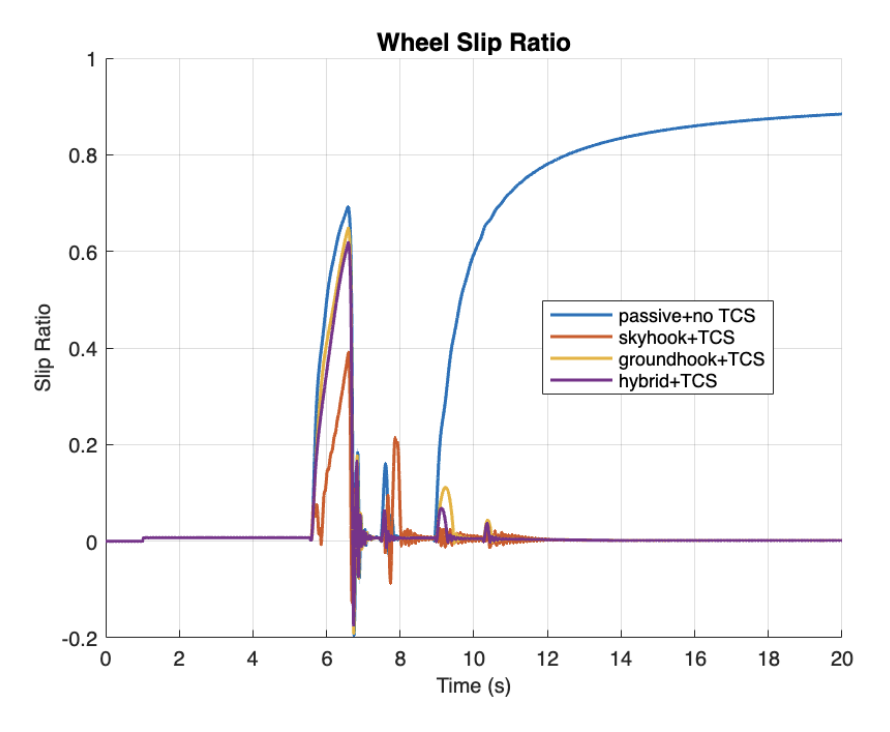


Figure 4.11: Four Bumps Road – Wheel Slip Ratio.

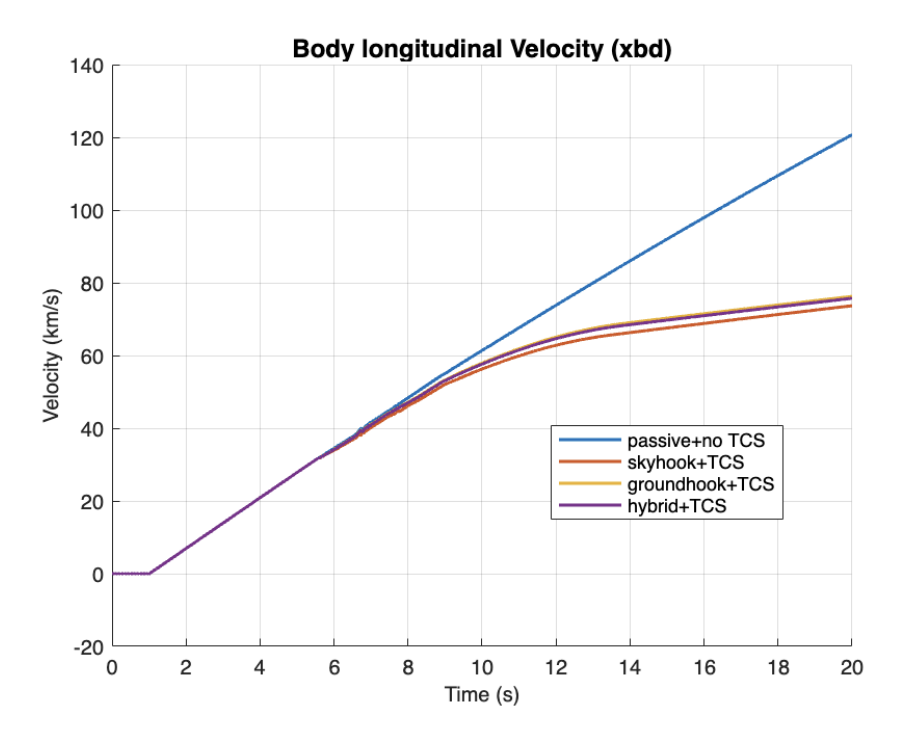


Figure 4.12: Four Bumps Road – Body Longitudinal Velocity (x_{bd}) .

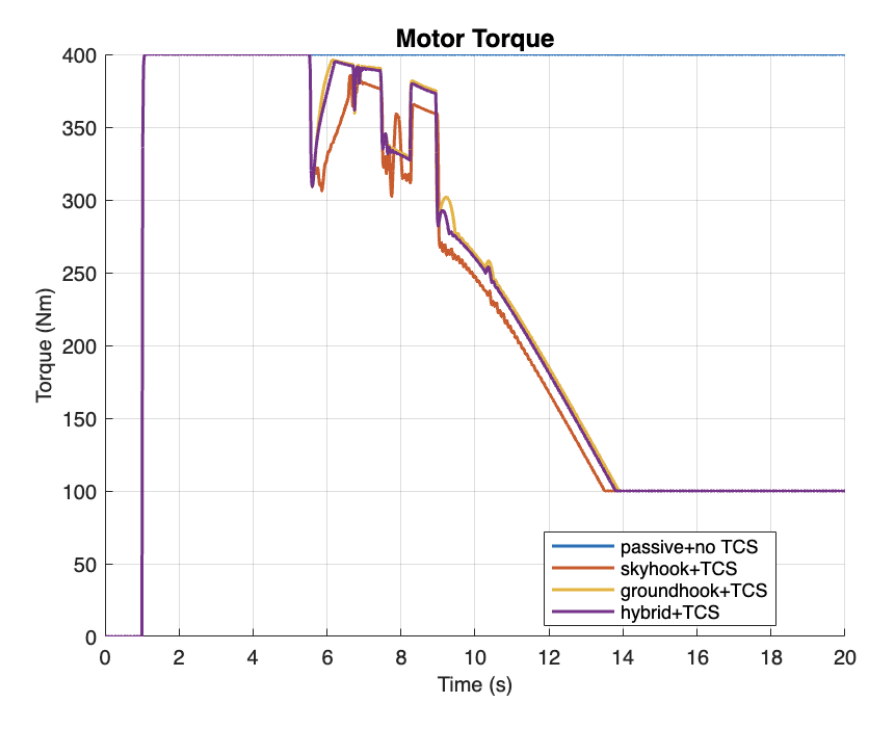
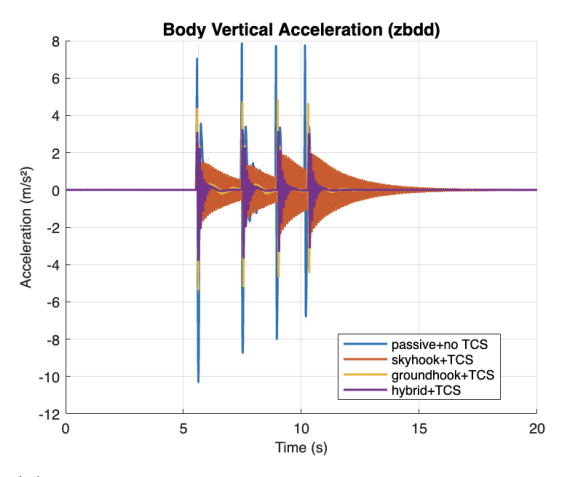
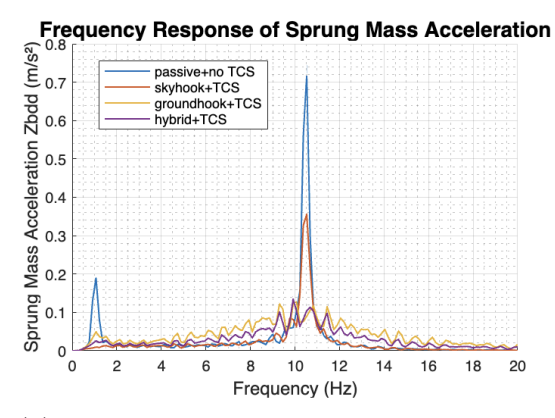


Figure 4.13: Four Bumps Road - Motor Torque.

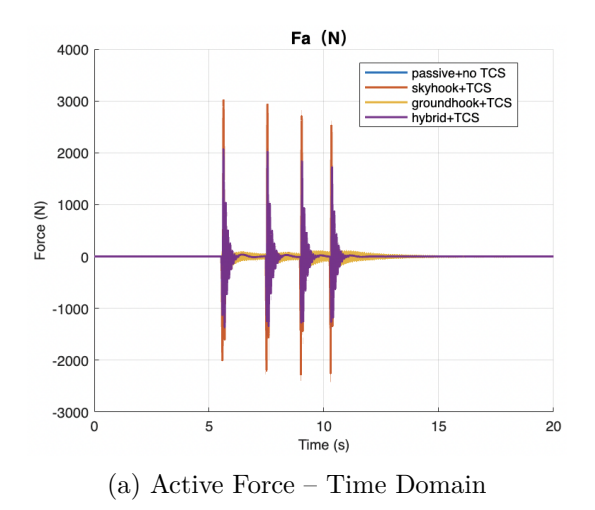


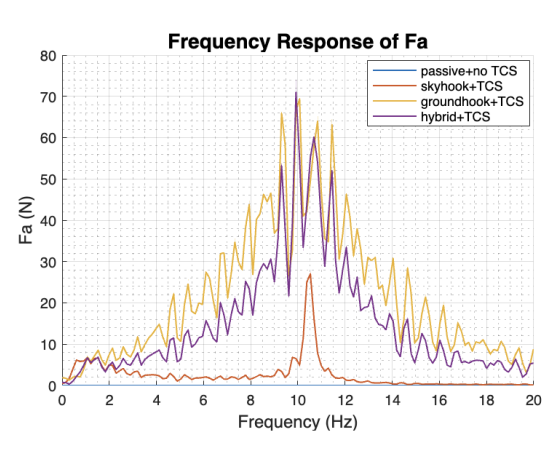


(a) Sprung Mass Acceleration – Time Domain

(b) Sprung Mass Acceleration – Frequency Domain

Figure 4.14: Four Bumps Road – Sprung Mass Acceleration.





(b) Active Force – Frequency Domain

Figure 4.15: Four Bumps Road – Active Force.

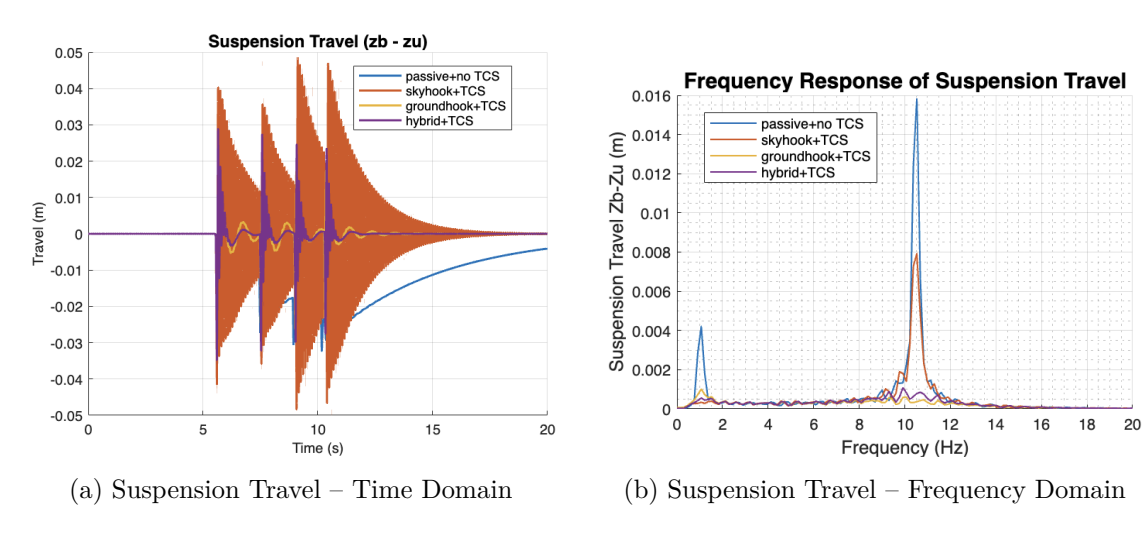


Figure 4.16: Four Bumps Road – Suspension Travel.

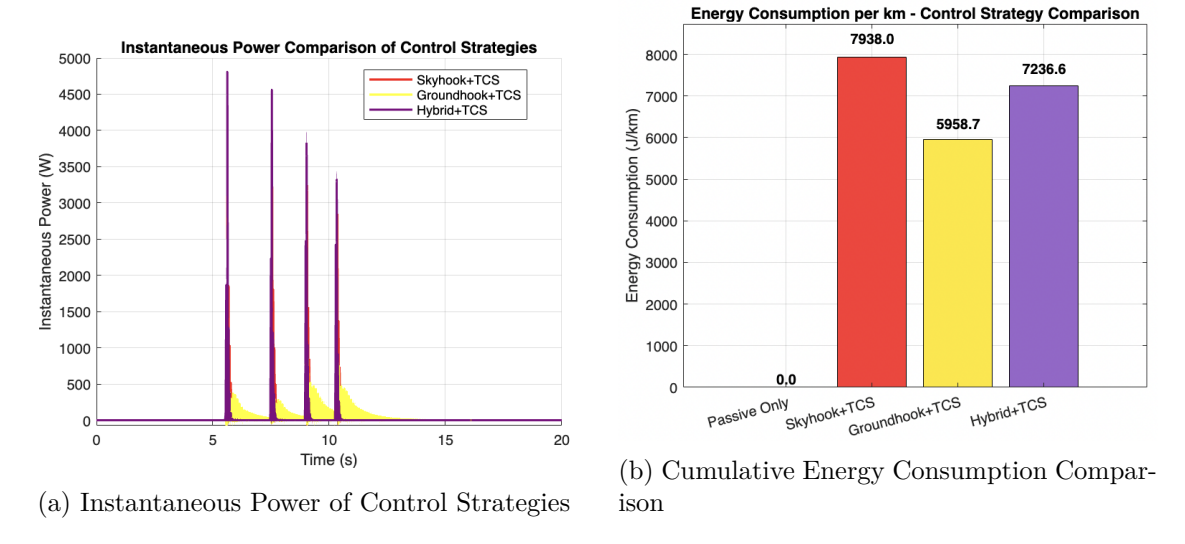


Figure 4.17: Four-bumps road – Power and Energy Consumption responses.

On the four-bumps road, the tendency is similar to the ISO road, Skyhook + TCS achieves the best comfort but consumes the most energy. Groundhook + TCS offers superior road holding and lowest energy use, while Hybrid + TCS maintains a balanced response between both aspects with lower amplitude and faster settle down time. In contrast with ISO road, The highest frequency response peak now can be found at wheel resonance frequency range around 10 Hz.

Chapter 5

Conclusion and Future Work

5.1 Summary of Findings

The analysis confirms that the additional unsprung mass introduced by in-wheel motors (IWMs) has a detrimental effect on vehicle dynamics. A larger unsprung mass amplifies vibrations transmitted to the sprung body and simultaneously reduces the ability of the tire to maintain consistent road contact. According to results from recent studies, this dual effect makes both the ride less comfortable and the driving more unstable.

The hybrid control approach, which combines Skyhook and Groundhook, applied with longitudinal slip control, strikes a good balance between three important goals: passenger comfort, road holding, and traction stability. This approach is suitable for in-wheel motor electric cars, as it addresses the unavoidable negative effects of extra unsprung mass.

The impact of road excitation was analyzed utilizing two representative profiles. The first type, an ISO-class road surface, can be represented as a stationary stochastic process, exhibiting a power spectral density (PSD) defined by predominant low-frequency components, approximately within the range of 0.5–2 Hz. The specified range aligns with the natural frequency of the human body in the vertical direction, resulting in increased sensitivity and average response in metrics related to comfort [13]. The four-bump road signifies a deterministic transient excitation. Each bump functions as a brief impulse that encompasses significant high-frequency content. The excitations are notably efficient in activating the unsprung mass resonance mode, generally found within the frequency range of 8–12 Hz, as indicated by the wheel–hop frequency approximation. The analysis indicates that the four-bump input induces a stronger excitation of this resonance, resulting in significant fluctuations in tire force and diminished stability.

In conclusion, the results show that (i) enhanced unsprung mass from IWMs degrades road holding and ride comfort, (ii) skyhook control mainly increases passenger comfort, (iii) groundhook control improves tire-road contact, (iv) the hybrid control approach is the most sensible and successful tactic. (v) longitudinal slip regulation guarantees stability in a range of road conditions, (vi) the comparison of stochastic (ISO road) and transient (four-bump) excitations shows that different management methods are needed depending on the road input's main frequency characteristics.

5.2 Future Research Directions

In IWM-based electric cars, this finding is a first step toward the coherent control of longitudinal and vertical dynamics. The suggested PID-based slip controller and Hybrid damping approach look good, but there is still a lot to learn about them.

5.2.1 Development of More Complex and High-Fidelity Vehicle Models

The built up quarter-car model offers useful insights; however, it does not possess the capability to account for lateral and coupled dynamic phenomena. Future efforts should concentrate on:

- Half-Car and Full-Vehicle Models: The integration of pitch and roll dynamics facilitates the analysis of load transfer occurring during acceleration, braking, and cornering maneuvers. Comprehensive vehicle models incorporate lateral dynamics, essential for evaluating combination maneuvers.
- Multi-Body Dynamics (MBD) Models: High-quality models developed in software such as ADAMS or Simpack can more precisely replicate suspension kinematics, flexible body influences, and tire-road interactions. These tools are suitable for validating and optimizing sophisticated control strategies in practical settings.

5.2.2 Advanced Control Techniques

Under simplified conditions, PID and Hybrid controllers demonstrate efficacy; however, it is important to investigate more sophisticated algorithms to augment their robustness.

- Nonlinear Model Predictive Control (NMPC): NMPC enables real-time synchronization of traction and ride comfort objectives by formulating a limited optimization problem based on nonlinear vehicle dynamics.
- Sliding Mode Control (SMC) and Adaptive Control: These approaches provide significant robustness in the presence of parameter uncertainty and external disruptions. They are especially appropriate for scenarios in which tire-road friction fluctuates.
- Learning-Based Approaches: Deep Reinforcement Learning (DRL) and datadriven adaptive controllers can ascertain optimal control techniques through simulation and subsequent real-world application.

5.2.3 Integrated Longitudinal and Vertical Dynamics Control

This study has analyzed longitudinal and vertical motions independently. The connection between these elements indicates that handling them collectively can lead to notable enhancements in performance:

- Unified Control Frameworks: Coordinated controllers that enhance longitudinal slip (σ) and vertical comfort $(a_{w,\text{rms}})$ concurrently can be created using multi-objective optimization.
- Predictive and Preview Control: Utilizing road preview data from onboard sensors (LiDAR, cameras) or V2X communication, the controller is capable of anticipating road conditions and proactively adjusting torque and damping.
- Multi-Objective Optimization: Advanced optimization techniques can effectively handle the balance between comfort, traction, and stability.

5.2.4 Experimental Validation and Real-Time Implementation

Relying solely on simulation studies for testing and validation may fails to deliver sufficient conclusive verification. Future research should concentrate on:

- Hardware-in-the-Loop (HIL) Testing: Testing algorithms in real-time on actual hardware ensures reliability and computational practicality before moving forward with on-road evaluations.
- Vehicle Experiments: On-road testing must be conducted across diverse driving and environmental conditions to validate improvements in comfort, stability, and safety.

5.2.5 Summary

This thesis highlights the challenges linked to increased unsprung mass in IWM-based electric vehicles and the potential of control strategies to address these problems. Future initiatives should focus on (i) enhancing model accuracy, (ii) investigating advanced and adaptable controllers, (iii) merging longitudinal and vertical dynamics into a cohesive framework, and (iv) conducting experimental validation. Addressing these aspects will contribute to the realization of safe, efficient, and comfortable IWM electric vehicles in practice.

Bibliography

- [1] Mehdi Ahmadian and Christopher Pare. A hybrid control strategy for semi-active vehicle suspensions. *Journal of Dynamic Systems, Measurement, and Control*, 123(1):109–116, 2001.
- [2] Ahmad Ammari, Moataz Hussein, and Olivier Sename. Nonlinear dynamics and braking control of in-wheel-motor electric vehicles. *Computers & Electrical Engineering*, 102:108276, 2022.
- [3] F. Belloni and et al. Tire slip control for electric vehicles: a review and perspective. *IEEE Transactions on Vehicular Technology*, 67(5):3904–3918, 2018.
- [4] Matej Biček, Tomaž Pepelnjak, and Franci Pušavec. Production aspect of direct drive in-wheel motors. In *Procedia CIRP*, volume 81, pages 1278–1283. Elsevier, 2019.
- [5] Chatchai Bunlapyanan and Hiroshi Fujimoto. Vertical force control of in-wheelmotor electric vehicles for ride comfort improvement. *IEEE Transactions on Indus*trial Electronics, 71(7):7651–7662, 2024.
- [6] J. D. Carlson and M. R. Jolly. Skyhook damping control theory and applications. *Vehicle System Dynamics*, 10(4):267–280, 1981.
- [7] IEEE CSS / CDC Benchmark Committee. Benchmark problem for motion control of four in-wheel motor actuated vehicles. Technical report, IEEE CSS / CDC Benchmark Committee, 2023. Accessed: 2025-09-30.
- [8] X. Gong, W. Chen, and K. Guo. Integrated control of traction and suspension systems for electric vehicles. *IEEE Transactions on Vehicular Technology*, 63(7):3039–3052, 2014.
- [9] Michael J. Griffin. Handbook of Human Vibration. Academic Press, London, 1990.
- [10] M. Guiggiani. Human exposure to whole-body vibration: Iso 2631 revisited. Journal of Sound and Vibration, 284(1-2):275–295, 2005.
- [11] D. Hrovat. Survey of advanced suspension developments and related optimal control applications. *Automatica*, 24(2):1781–1817, 1988.

- [12] D. Hrovat. Survey of advanced suspension developments and related optimal control applications. *Automatica*, 33(10):1781–1817, 1997.
- [13] International Organization for Standardization. Mechanical vibration road surface profiles reporting of measured data, 1995. ISO 8608.
- [14] International Organization for Standardization. Mechanical vibration and shock evaluation of human exposure to whole-body vibration, 1997. ISO 2631.
- [15] Dean Karnopp, M. J. Crosby, and R. A. Harwood. Vibration control using semi-active force generators. *Journal of Engineering for Industry*, 96(2):619–626, 1974.
- [16] Pengfei Li, Tao Wang, Lei Zhang, and Wei Li. Performance study of vehicle suspension control strategies based on frequency-domain analysis. *Journal of Automotive Engineering*, 21(16):016, 2024.
- [17] D. Millet and D. Hrovat. Vehicle road-holding and ride comfort trade-offs in semi-active suspensions. *Vehicle System Dynamics*, 25(5):367–382, 1996.
- [18] Anh Tuan Nguyen, Alain Bouscayrol, and Wilfrid Lhomme. Longitudinal dynamics modeling of in-wheel-motor electric vehicles. *IEEE Transactions on Vehicular Technology*, 69(6):5740–5751, 2020.
- [19] Hans B. Pacejka. Tire and Vehicle Dynamics. SAE International, Warrendale, PA, USA, 1996.
- [20] G. Raffo, F. Milano, and A. Rizzo. Semi-active suspension control: a survey and recent advances. *Journal of Dynamic Systems, Measurement, and Control*, 136(6):061001, 2014.
- [21] Rajesh Rajamani. Vehicle dynamics and control. Springer Science & Business Media, 2011.
- [22] Ryan Samaroo, Jie Wang, and Min Liao. Semi-active suspension with dual vibration absorbers for in-wheel-motor electric vehicles. *Mechanical Systems and Signal Processing*, 210:111512, 2025.
- [23] Zhihua Shi, Zhuoping Yu, and Lin Chen. Investigation of negative influences on ride comfort performance of in-wheel motor vehicles with high unsprung mass. *Proceedings of the Institution of Mechanical Engineers, Part D: Journal of Automobile Engineering*, 229(3):290–303, 2015.
- [24] Víctor Vidal, Pietro Stano, Gaetano Tavolo, Miguel Dhaens, Davide Tavernini, Patrick Gruber, and Aldo Sorniotti. On pre-emptive in-wheel motor control for reducing the longitudinal acceleration oscillations caused by road irregularities. *IEEE Transactions on Vehicular Technology*, 71(9):9322–9337, 2022.
- [25] Jiaqi Wu, Wei Zhang, and Wei Sun. Effects of in-wheel-motor unsprung mass on ride comfort and handling stability. *Vehicle System Dynamics*, 62(5):873–892, 2024.

[26] Wei Zhang, Yan Liu, Pengfei Wang, and Jian Li. A robust slip based traction control of electric vehicle under different road conditions. *International Journal of Automotive Technology*, 17(1):151–158, 2016.